

# Quantum-enhanced mean value estimation via adaptive measurement

Kaito Wada,<sup>1,\*</sup> Kazuma Fukuchi,<sup>1</sup> and Naoki Yamamoto<sup>1,2,†</sup>

<sup>1</sup>*Department of Applied Physics and Physico-Informatics, Keio University,  
3-14-1 Hiyoshi, Kohoku-ku, Yokohama, Kanagawa, 223-8522, Japan*

<sup>2</sup>*Quantum Computing Center, Keio University, 3-14-1 Hiyoshi,  
Kohoku-ku, Yokohama, Kanagawa, 223-8522, Japan*

Quantum-enhanced (i.e., less query complexity compared to any classical method) mean value estimation of observables is a fundamental task in various quantum technologies; in particular, it is an essential subroutine in quantum computing algorithms. Notably, the quantum estimation theory identifies the ultimate precision of such estimator, which is referred to as the quantum Cramér-Rao (QCR) lower bound or equivalently the inverse of the quantum Fisher information. Because the estimation precision directly determines the performance of those quantum technological systems, it is highly demanded to develop a generic and practically implementable estimation method that achieves the QCR bound. Under imperfect conditions, however, such ultimate estimator has not been developed. This paper proposes a quantum-enhanced mean value estimation method in a depolarizing noisy environment that asymptotically achieves the QCR bound exponentially fast with respect to the number of qubits. The method employs a maximum likelihood estimator consisting of the amplitude amplification and an implementable measurement, which are adaptively optimized to achieve the QCR bound. We provide a rigorous analysis for the statistical properties of the proposed adaptive estimator such as consistency and asymptotic normality. Furthermore, several numerical simulations are provided to demonstrate the effectiveness of the method, particularly showing that the estimator needs only a modest number of measurements to almost saturate the QCR bound. The proposed method will be useful in various applications beyond the subroutine in quantum computing algorithms, thereby paving the way for an interdisciplinary research in quantum computing and quantum sensing.

## I. INTRODUCTION

Mean value estimation of quantum observables is an important task in many quantum information technologies, such as subroutines in quantum algorithms for both near-term noisy and future fault-tolerant quantum devices. For instance, variational quantum algorithms require estimating mean values iteratively to train the parameters of a parameterized quantum circuit [1–13]. Surely, the performance of those information processing technologies heavily depends on the estimation precision. In addition, real quantum devices suffer from noise induced by the interaction of system and environment, and such noise deteriorates the efficiency for reading out calculation results. Therefore, developing efficient mean-value estimation methods (in a noisy environment) is highly important [14–20].

For this purpose, the statistical estimation theory [21, 22] and their quantum extension [23, 24] are useful. In particular, the seminal Cramér-Rao inequality and Fisher information, which identify the limit of estimation precision, have been extended to quantum versions [24–28]; that is, the quantum Cramér-Rao (QCR) inequality and quantum Fisher information. Actually, as in the classical case, they can be used to determine the ultimate performance of several quantum information processing systems such as quantum sensors [29–32]. Moreover, the

QCR casts as a fundamental limitation on information extractable from quantum mechanical systems, e.g., [33]. Therefore, extensive investigations have been conducted to characterize estimators that (almost) achieve the ultimate precision limit i.e., the QCR bound [34–41]. Note that, in most cases, such optimal estimators are not physically implementable, because they depend on the target quantity to be estimated; devising an implementable and optimal (in the sense of QCR) estimator is thus one of the most important subjects in quantum sensing.

In this way, the quantum statistical estimation theory should be appropriately applied to develop estimators for various quantities including mean-values of quantum observables, which appear in quantum computing. This exploration has just started recently, and we find only a few such trials. For instance, some less-demanding implementation methods for the quantum-enhanced (i.e., less query complexity compared to any classical means) phase estimation algorithm [42–45] and amplitude estimation algorithm [46–56] have been developed, and their performance have been investigated in depth using statistical estimation theory, yet without studying the QCR bound. Moreover, Ref. [18] formulated the mean-value estimation problem within the framework of amplitude estimation and proposed a Bayesian inference method for this problem; however, again, there was no discussion on how to achieve the QCR bound. To our best knowledge, only Ref. [53] gave a detailed analysis on the QCR bound in the quantum amplitude estimation problem; in particular, under the assumption that the system is subjected to depolarization noise, the estimator given in [53] achieves the precision that is yet strictly lower than the

---

\* wkai1013keio840@keio.jp

† yamamoto@appi.keio.ac.jp

ultimate limit. Thus, the following questions naturally arise. (i) For the quantum mean value estimation problem under noisy environment, is there an estimator such that the estimation precision achieves the QCR bound? (ii) If exists, can the estimator, especially the measurement process, be explicitly implemented? (iii) Also, is there any mathematical guarantee on the estimation performance?

This paper gives positive answers to all the above questions. Answering the question (i), we develop a quantum-enhanced mean-estimation method that asymptotically achieves the QCR bound, under noisy environment assuming the depolarizing channel. This method uses a modified maximum likelihood estimator that adaptively optimizes the measurement (positive operator-valued measure (POVM)) and the number of amplitude amplification operations, based on the quantum Fisher information; as a result, the estimator asymptotically achieves the QCR bound exponentially fast with respect to the number of qubits, which is supported by Theorem 1 presented in Section III. Note that, as mentioned in the second paragraph, in general such an optimal measurement is not given as a physically-implementable form, but in our case it can be efficiently implemented on a standard quantum computing device, which thus answers to the question (ii). As for the question (iii), we actually prove that the estimator satisfies the following statistical properties.

- Consistency (Theorem 2): As the number of measurements increases, the estimation accuracy becomes better. More precisely, the probability that the estimated value is arbitrarily close to the true value approaches 1 in the infinite limit of the number of measurements.
- Asymptotic normality (Theorem 3): The estimator regularized by its Fisher information asymptotically follows the standard normal distribution, as the number of measurements increases. As a result, the estimation error asymptotically achieves the classical Cramér-Rao lower bound.

Therefore the proposed estimator has mathematical guarantees in its performance.

In addition to the above theoretical contributions, Section IV is devoted to thorough numerical simulations. In particular, we will demonstrate that the above asymptotic properties hold even with a modest number of each measurement ( $\sim 500$ ) and a modest number of qubits ( $\sim 20$ ). Also, we focus on the previously-reported problem that the precision of the quantum mean value estimation under the depolarizing noise may significantly deteriorate depending on the target value to be estimated; but we will numerically demonstrate that the proposed method can also get around this problem due to the optimization. Note here that the above-mentioned Bayesian inference method [18] optimizes a quantum circuit containing multi-parameter in order to alleviate the

target value dependency of estimation efficiency, while our method optimizes just one discrete parameter, which is clearly computationally advantageous.

## II. PRELIMINARY

The quantum-enhanced amplitude estimation algorithm studied in [47, 52, 53, 55], which does not use the hard-to-implement phase estimation algorithm, consists of two major steps. The first step is to perform amplitude amplification on the quantum state whose amplitude is to be estimated, and then make a measurement; this procedure is repeated with different operation times. The second step is to estimate the amplitude by classical post-processing for the combined measurement result, i.e., the maximum likelihood estimation.

The problem is to estimate the amplitude  $\sin(\phi^*)$ , with unknown  $\phi^* \in [0, \pi/2]$ , of the following  $(n+1)$ -qubit quantum state  $\mathcal{A}|0\rangle_{n+1}$ :

$$\mathcal{A}|0\rangle_{n+1} := \cos(\phi^*)|\psi_0\rangle_n|0\rangle_1 + \sin(\phi^*)|\psi_1\rangle_n|1\rangle_1, \quad (1)$$

where  $|0\rangle_{n+1}$  is the computational basis of  $(n+1)$ -qubit. Here,  $\mathcal{A}$  is a unitary operator whose action is defined as Eq. (1), and  $|\psi_0\rangle_n$  and  $|\psi_1\rangle_n$  are normalized  $n$ -qubit quantum states. The first step is to amplify the amplitude via the operator  $\mathcal{Q}$  defined as

$$\mathcal{Q} := \mathcal{A}(2|0\rangle_{n+1}\langle 0|_{n+1} - I_{n+1})\mathcal{A}^\dagger(I_n \otimes Z), \quad (2)$$

where  $I_n$  is the identity operator on the  $n$ -qubit system, and  $Z$  denotes the  $2 \times 2$  Pauli  $Z$  matrix. When  $\mathcal{Q}$  is applied  $m$  times to the state (1), we obtain [14]

$$\begin{aligned} \mathcal{Q}^m \mathcal{A}|0\rangle_{n+1} &= \cos[(2m+1)\phi^*]|\psi_0\rangle_n|0\rangle_1 \\ &+ \sin[(2m+1)\phi^*]|\psi_1\rangle_n|1\rangle_1. \end{aligned} \quad (3)$$

We now measure the last qubit of Eq. (3) by the computational basis  $|0\rangle_1$  and  $|1\rangle_1$ . Then the probability of obtaining "1" is given by

$$\tilde{\mathbf{P}}(m; \phi^*) := \frac{1}{2} - \frac{1}{2} \cos[2(2m+1)\phi^*]. \quad (4)$$

Note that this is equivalent to the Bernoulli trials with success probability  $\tilde{\mathbf{P}}(m; \phi^*)$ .

In the second step we estimate the amplitude based on the measurement results obtained in the first step by the maximum likelihood estimation method. For each of predefined odd numbers  $2m_k + 1$  ( $k = 1, 2, \dots, M$ ), we prepare the state (3) and measure it  $N$  times with the computational basis independently. Here,  $M$  denotes the total number of types of quantum states to be prepared. We write  $x^{(k)} \in \{0, 1, \dots, N\}$  as the number of hitting "1" for the state  $\mathcal{Q}^{m_k} \mathcal{A}|0\rangle_{n+1}$ . The measurement results for  $M$  different states are put together as  $\mathbf{x}_M := (x^{(1)}, x^{(2)}, \dots, x^{(M)})$ . Then the likelihood function to have  $\mathbf{x}_M$  is given by

$$\tilde{\mathcal{L}}_M(\phi; \mathbf{x}_M) := \prod_{k=1}^M \tilde{F}_k(x^{(k)}; m_k, \phi), \quad (5)$$

where  $\tilde{F}_k(x^{(k)}; m_k, \phi^*)$  is the probability of obtaining  $x^{(k)}$ . Given the measurements  $\mathbf{x}_M$ , the maximum likelihood estimation assumes that the value of  $\phi$  that maximizes  $\tilde{\mathcal{L}}_M(\phi; \mathbf{x}_M)$  is a plausible estimate of the true value  $\phi^*$ . In other words, the maximum likelihood estimate  $\hat{\phi}_M$  for  $\phi^*$  from the  $M$  series of measurements is defined as

$$\hat{\phi}_M := \operatorname{argmax}_{\phi \in [0, \pi/2]} \tilde{\mathcal{L}}_M(\phi; \mathbf{x}_M). \quad (6)$$

Note that the maximum likelihood estimator for  $\sin(\phi^*)$  corresponds to  $\sin(\hat{\phi}_M)$  due to the invariance property of maximum likelihood estimators. Thanks to the amplitude amplification, the estimation precision of  $\phi^*$  and  $\sin(\phi^*)$  can be improved quadratically with respect to the number of total queries, by using a specific sequence  $m_k = 2^{k-1}$  as demonstrated in [47].

We now consider the  $n$ -qubit depolarizing channel:

$$\mathcal{D}[\rho] := p\rho + \frac{1-p}{d}I_n, \quad d := 2^n, \quad (7)$$

where  $\rho$  is an arbitrary density operator and  $1-p$  is the probability that depolarization occurs. In this paper, as in [18, 52, 53], we consider a noise model in which depolarization occurs with probability  $1-p_s$  for state preparation and  $1-p_q$  for each amplitude amplification. Then the probability of obtaining "1" for the final state under this noise model is given by

$$\tilde{\mathbf{P}}_{\mathcal{D}}(m; \phi^*) := \frac{1}{2} - \frac{p_s p_q^m}{2} \cos[2(2m+1)\phi^*]. \quad (8)$$

The subscript  $\mathcal{D}$  means that the quantum state to be measured has passed through the above-defined depolarizing channels. Then the classical Fisher information associated with the probability (8) for  $\phi^*$  is calculated as

$$\tilde{\mathcal{I}}_c(m; \phi^*) := \frac{(2m+1)^2 (p_s p_q^m)^2 \sin^2[2(2m+1)\phi^*]}{\tilde{\mathbf{P}}_{\mathcal{D}}(m; \phi^*) (1 - \tilde{\mathbf{P}}_{\mathcal{D}}(m; \phi^*))}. \quad (9)$$

Equation (9) indicates that the estimation may become ineffective if  $m$  satisfies  $\sin[2(2m+1)\phi^*] \simeq 0$ . More precisely, if  $m$  and  $\phi^*$  satisfy this condition, the classical Cramér-Rao lower bound of the estimation error for  $\phi^*$  significantly deteriorates [18, 52]. In addition, even if we use the above-described maximum likelihood estimation based on the  $M$  series of measurements for  $m_k$  ( $k = 1, 2, \dots, M$ ), which are predefined independently to  $\phi^*$ , the same deterioration may occur [52]. Importantly, this phenomena are also seen in the quantum mean value estimation problem discussed in the next section.

### III. QUANTUM-ENHANCED MEAN VALUE ESTIMATION

#### A. Amplitude amplification and measurement

Our goal is to estimate the mean value of a Hermitian operator  $\mathcal{O}$  with eigenvalues  $\pm 1$ , i.e.,  $\langle \mathcal{O} \rangle :=$

$\langle A | \mathcal{O} | A \rangle$ , where  $|A\rangle := A|0\rangle_n$  is an  $n$ -qubit quantum state with a unitary operator  $A$ . The amplitude estimation method described in the previous section can be applied to this problem; hence, ideally, we need quadratically less queries compared to the standard algorithm without amplitude amplification, to estimate the mean value with specified estimation error — that is, the quantum-enhanced mean value estimation. A typical  $\mathcal{O}$  is a single Pauli string such as  $\mathcal{O} = X \otimes Z \otimes \dots$ ; note that our method is applicable to estimate the mean value of a linear combination of Pauli strings that form a completely anti-commuting set, because there exists a unitary operator that groups the linear combination into a single Pauli string [57].

Suppose  $|A\rangle$  is not an eigenstate of  $\mathcal{O}$  (thus  $|\langle \mathcal{O} \rangle| \neq 1$ ) and that the two quantum states  $|A\rangle$  and  $\mathcal{O}|A\rangle$  are linearly independent and form the following subspace [18, 58]:

$$\mathcal{S} := \operatorname{Span}\{|A\rangle, \mathcal{O}|A\rangle\} = \operatorname{Span}\{|A\rangle, |A^\perp\rangle\}, \quad (10)$$

where  $|A^\perp\rangle$  is a normalized state orthogonal to  $|A\rangle$  obtained by Gram-Schmidt procedure to  $|A\rangle$  and  $\mathcal{O}|A\rangle$ . We denote  $|A\rangle$  and  $|A^\perp\rangle$  as  $|\bar{0}\rangle$  and  $|\bar{1}\rangle$ , respectively, and identify  $\mathcal{S}$  as the 1-qubit Hilbert space likewise the idea of qubitization [59]. We then define an  $n$ -qubit operator  $Q$  on  $\mathcal{S}$ , which corresponds to the amplitude amplification operator in Eq. (2), as

$$Q := A(2|0\rangle_n \langle 0|_n - I_n)A^\dagger \mathcal{O}. \quad (11)$$

This operator keeps the subspace  $\mathcal{S}$  invariant. Now the representation of  $Q$  on  $\mathcal{S}$  is expressed as  $Q|_{\mathcal{S}} = R_{\bar{Y}}(-2\theta^*)$ , where  $\bar{Y}$  is the Pauli  $Y$  matrix in the basis  $|\bar{0}\rangle$  and  $|\bar{1}\rangle$ , and  $\theta^* := \arccos(\langle \mathcal{O} \rangle)$ . Note that, for the target mean value  $\langle \mathcal{O} \rangle = \cos\theta^*$ , the domain of  $\theta^*$  is given by  $\theta^* \in (0, \pi)$ , which is twice as that of  $\phi^*$  in the previous section. Acting  $Q$  on  $|A\rangle$   $m$  times yields

$$\begin{aligned} Q^m |A\rangle &= (Q|_{\mathcal{S}})^m |\bar{0}\rangle \\ &= \cos(m\theta^*)|\bar{0}\rangle - \sin(m\theta^*)|\bar{1}\rangle. \end{aligned} \quad (12)$$

Here, as in the previous case, we assume that the state is subjected to the depolarization noise through the amplitude amplification process; that is, the output state after  $m$  repetition of  $Q$  is given by

$$\rho_{\mathcal{D}}(m; \theta^*) := p_s p_q^m \rho(m; \theta^*) + \frac{1 - p_s p_q^m}{d} I_n, \quad (13)$$

where  $\rho(m; \theta^*) := Q^m |A\rangle \langle A| (Q^m)^\dagger$ . Here,  $1 - p_q (> 0)$  denotes the probability of depolarization noise occurring along the single query of the operator  $Q$ .

To best efficiently read out the quantum mean value from the noisy amplitude-amplified quantum state (13), we need a POVM whose classical Fisher information achieves the quantum Fisher information defined for this state; see Appendix A for a summary of this theory. In fact, we found a 3-valued POVM that satisfies the above

requirement for specific values of  $\theta^*$ ; but the implementation of this POVM on standard quantum computing devices is highly nontrivial (See Appendix B). Hence we approximate the ideal 3-valued POVM by marginalizing it, to have the following 2-valued POVM:

$$\begin{aligned} M_1^{(\text{even})} &:= I_n - M_0^{(\text{even})}, \\ M_0^{(\text{even})} &:= \mathcal{O}^\dagger |A\rangle \langle A| \mathcal{O}, \end{aligned} \quad (14)$$

where the meaning of *even* is explained later. The derivation is given in Appendix B. Note that this POVM can be implemented by operating  $A^\dagger \mathcal{O}$  on the state (12) to prepare  $A^\dagger \mathcal{O} Q^m |A\rangle$ , followed by the computational basis measurement and post-processing for classifying the obtained measurements into "0" or "1".

This measurement (14) has powerful estimation capabilities in the sense of its Fisher information, as follows. Measuring the state (13) with this POVM, we obtain the result corresponding to  $M_1^{(\text{even})}$  with probability

$$\begin{aligned} \mathbf{P}_{\mathcal{D}}^{(\text{even})}(m; \theta^*) \\ := \frac{d-1}{d} + p_s p_q^{m+1/2} \left[ \sin^2 [(m+1)\theta^*] - \frac{d-1}{d} \right], \end{aligned} \quad (15)$$

where  $p_q^{1/2}$  denotes the additional noise occurring with  $A^\dagger$  for implementing the POVM. The classical Fisher information per shot with Eq. (15) can be calculated as

$$\begin{aligned} \mathcal{I}_c^{(\text{even})}(m; \theta^*) \\ := \frac{(2m+2)^2 p_s^2 p_q^{2m+1} \sin^2 [(2m+2)\theta^*]}{4 \mathbf{P}_{\mathcal{D}}^{(\text{even})}(m; \theta^*) \left( 1 - \mathbf{P}_{\mathcal{D}}^{(\text{even})}(m; \theta^*) \right)}. \end{aligned} \quad (16)$$

Also we can calculate the quantum Fisher information using the standard recipe found in e.g., [60, 61]:

$$\mathcal{I}_q^{(\text{even})}(m) := \frac{(p_s p_q^{m+1/2})^2}{\frac{2}{d} + \left(1 - \frac{2}{d}\right) p_s p_q^{m+1/2}} (2m+2)^2. \quad (17)$$

Importantly, when  $\cos[(m+1)\theta^*] \neq 0$ , the classical Fisher information approaches the quantum Fisher information exponentially fast with respect to the number of qubits, as follows.

**Theorem 1.** (Optimality of the marginalized POVM)

$$\mathcal{I}_c^{(\text{even})}(m; \theta^*) = \kappa \mathcal{I}_q^{(\text{even})}(m) + O\left(\frac{1}{2^n(1-\kappa)}\right) \quad (18)$$

holds, where  $\kappa \in [0, 1)$  is defined as

$$\kappa := \frac{\sin^2 [(m+1)\theta^*]}{1 - p_s p_q^{m+1/2} \cos^2 [(m+1)\theta^*]}. \quad (19)$$

When  $\theta^*/2\pi$  is an irrational number, there exists an  $m$  (i.e., the number of querying  $Q$ ) such that  $\kappa$  is arbitrarily close to 1.

This theorem means that, to estimate a *particular*  $\theta^*$ , the POVM (14) can become optimal in the sense of Fisher information, as the number of qubits increases; additional analysis is provided in Appendix B. Note that the trade-off between the first and second terms in Eq. (18) in terms of  $\kappa$  stems from the cost of taking marginalization on the original 3-valued POVM for implementation. Based on this theorem, in the next subsection we introduce an algorithm that optimizes  $m$  within a certain finite range and thereby achieves  $\kappa \approx 1$ . This optimization is often valid even when  $\theta^*/2\pi$  is a rational number as demonstrated later. As a consequence, this algorithm enables us to have an optimal POVM for *almost all*  $\theta^*$  in the large system dimension, in the sense of Fisher information (more precisely the total Fisher information defined later).

Although the even POVM (14) can become optimal in the sense of Fisher information, this does not necessarily guarantee that the actual estimator (particularly the maximum likelihood estimator based on the POVM) produces the best estimate that achieves the QCR bound. Actually, the probability (15) is an even function with respect to the value  $\theta^* - \pi/2$ , and the maximum likelihood estimation associated with this even POVM cannot distinguish the sign of mean values. To construct an estimator that may correctly estimate the true target value, we therefore introduce the following second POVM that breaks the above-mentioned symmetry:

$$\begin{aligned} M_1^{(\text{odd})} &:= I_n - M_0^{(\text{odd})}, \\ M_0^{(\text{odd})} &:= \frac{I_n + \mathcal{O}}{2}. \end{aligned} \quad (20)$$

This POVM corresponds to Eq. (8) in the standard amplitude estimation algorithm, because the probability of obtaining "1" by measuring the state (13) with the POVM (20) is given as

$$\mathbf{P}_{\mathcal{D}}^{(\text{odd})}(m; \theta^*) = \frac{1}{2} - \frac{p_s p_q^m}{2} \cos [(2m+1)\theta^*]. \quad (21)$$

The coefficient of  $\theta^*$  differs by the factor 2 compared to that of  $\phi^*$  in Eq. (8), because the presence of sign for quantum mean values doubles the domain of the target value. Since the probability (21) is an odd function unlike Eq. (15), the measurement can distinguish the sign of the target mean value. For this reason, we have added the superscript *even* or *odd* for the POVMs (14) and (20). Note that, in contrast to the even POVM, the classical Fisher information corresponding to the odd POVM,  $\mathcal{I}_c^{(\text{odd})}(m; \theta^*)$ , always deviates from the quantum Fisher information even if the number of qubits increases; see Appendix B.

Hence, our estimator is composed of the even and odd POVMs, where the probability of obtaining the measure-

ment result "1" is summarized as follows:

$$\mathbf{P}_{\mathcal{D}}(\alpha; \theta^*) := \begin{cases} \frac{1}{2} - \frac{\eta_{\alpha}}{2} \cos(\alpha\theta^*), & \alpha \text{ is odd} \\ \frac{d-1}{d} + \eta_{\alpha} \left[ \sin^2\left(\frac{\alpha}{2}\theta^*\right) - \frac{d-1}{d} \right], & \alpha \text{ is even} \end{cases}. \quad (22)$$

Here  $\eta_{\alpha} = p_s p_q^{\frac{\alpha-1}{2}}$  and  $\alpha \in \mathbb{N}$  represents the number of queries of the operator  $A$  and  $A^{\dagger}$ . We perform the measurement via Eq. (20) when  $\alpha$  is odd ( $\alpha = 2m + 1$ ) and via Eq. (14) when  $\alpha$  is even ( $\alpha = 2m + 2$ ). In the following, we call  $\alpha$  the *amplified level*. Also, the classical/quantum Fisher information corresponding to each measurement is represented as

$$\mathcal{I}_c(\alpha; \theta^*) := \frac{\alpha^2 \eta_{\alpha}^2 \sin^2(\alpha\theta^*)}{4\mathbf{P}_{\mathcal{D}}(\alpha; \theta^*)(1 - \mathbf{P}_{\mathcal{D}}(\alpha; \theta^*))}, \quad (23)$$

$$\mathcal{I}_q(\alpha) := \frac{\alpha^2 \eta_{\alpha}^2}{\frac{2}{d} + (1 - \frac{2}{d}) \eta_{\alpha}}. \quad (24)$$

To estimate the mean value  $\langle \mathcal{O} \rangle = \cos\theta^*$ , we take the maximum likelihood estimation method combined with the above-described amplitude amplification and POVMs.

### B. The proposed adaptive mean-value estimation algorithm

When  $\sin(\alpha\theta^*) \simeq 0$ , the classical Fisher information (23) becomes nearly zero, and thus the estimation becomes inefficient by the Cramér-Rao inequality. Hence, such  $\alpha$  should be avoided, in both POVMs (14) and (20). At the same time, we want to employ measurements whose classical Fisher information approaches the quantum Fisher information for enhancing the estimation power. Here we provide a mean value estimation method that adaptively adjusts the amplified level  $\alpha$  and thereby satisfies these two requirements. Importantly, this method inherits several good properties of the maximum likelihood estimation, as proven in Section III. C. Note that, in the context of the amplitude estimation algorithms described in Section II, Ref. [53] discusses the similar POVM in Eq. (14). However, unlike our method, the algorithm of [53] does not employ an adaptive optimization algorithm for estimation; thus it cannot achieve the quantum Fisher information for almost all  $\theta^*$  and also suffers from the problem of vanishing classical Fisher information.

Our algorithm is based on the maximum likelihood estimation method for the random variables subjected to the probability distribution (22). An overview is shown in Fig. 1. The algorithm is composed of the following four steps.

- (i) Identify the probabilities of depolarization  $1 - p_s$  and  $1 - p_q$  by some experiments on the quantum device to be used. For the first measurement, we set the amplified level as  $\alpha_1 = 1$ .

Unlike Bayesian estimation, our algorithm does not require any prior information on the target value.

- (ii) Measure the quantum state (13)  $N$  times independently with either POVM (14) or (20), according to the amplified level  $\alpha_k$ . We write the total number of hitting "1" as  $x^{(k)} \in \{0, 1, \dots, N\}$ . Here,  $x^{(k)}$  is a realization of the Binomial random variable

$$X^{(k)} \sim \text{Bin}(N, \mathbf{P}_{\mathcal{D}}(\alpha_k; \theta^*)). \quad (25)$$

- (iii) Calculate the maximum likelihood estimate  $\hat{\theta}_k$  based on the total  $k$  measurement results  $\mathbf{x}_k := (x^{(1)}, x^{(2)}, \dots, x^{(k)})$ . That is,  $\hat{\theta}_k$  maximizes the likelihood function

$$\mathcal{L}_k(\theta; \mathbf{x}_k) := \prod_{m=1}^k F_m(x^{(m)}; \alpha_m(\mathbf{x}_{m-1}), \theta), \quad (26)$$

where  $F_m(x^{(m)}; \alpha_m(\mathbf{x}_{m-1}), \theta)$  is the probability distribution of the random variable  $X^{(m)}$ .

Note that the measurements  $\mathbf{x}_k$  is the collection of all the results via the measurements with  $\alpha_m$  ( $m = 1, 2, \dots, k$ ). Since the amplified level  $\alpha_k$  depends on the previous results  $\mathbf{x}_{k-1}$  as described below (except for the case  $k = 1$ ), the likelihood function  $\mathcal{L}_k(\theta; \mathbf{x}_k)$  has a hierarchical structure, unlike the case of Eq. (5).

- (iv) To enhance the classical Fisher information, determine  $\alpha_{k+1}$  for the next measurement based on the current estimate  $\hat{\theta}_k$  by numerically solving the following optimization problem:

$$\alpha_{k+1} := \underset{\alpha \in D_k}{\text{argmax}} \frac{\mathcal{I}_c(\alpha; \hat{\theta}_k)}{\mathcal{I}_q(\alpha)} \frac{\sin^2(\alpha\hat{\theta}_k)}{1 - \delta \cos^2(\alpha\hat{\theta}_k)}, \quad (27)$$

where  $D_k$  is the finite range in  $\mathbb{N}$ . Then return to (ii) and perform the measurement again.

Here,  $\delta \in (0, 1]$  is a parameter for regularization as detailed below. Since the elements of  $D_k$  are integer, the optimization problem can be efficiently solved using a simple brute force method. In the case  $\delta = 1$ , the optimization corresponds to maximizing the ratio between the classical and quantum Fisher information, where the maximum value of the ratio is 1 because of the quantum Cramér-Rao inequality  $\mathcal{I}_c(\alpha; \hat{\theta}_k) \leq \mathcal{I}_q(\alpha)$  [24–28].

We here describe the role of the regularization which is multiplied by the ratio of Fisher information in Eq. (27). The key is Theorem 1, stating that, when  $\alpha$  is even and  $d = 2^n$  is sufficiently large, the optimization with  $\delta = 1$  is equivalent to maximizing  $\kappa$  given in Eq. (19) for the current estimate  $\hat{\theta}_k$ . Then, by further requiring  $\theta^*/2\pi$  to be

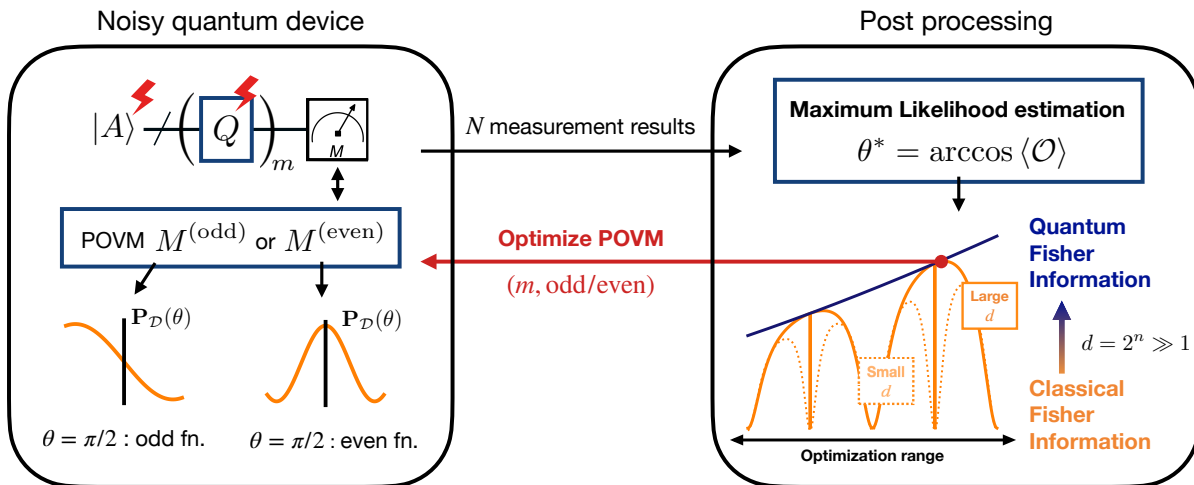


FIG. 1. Overview of the proposed algorithm for estimating  $\langle \mathcal{O} \rangle = \langle A | \mathcal{O} | A \rangle$ . Here,  $|A\rangle$  is a target state prepared by operating an  $n$ -qubit quantum circuit  $A$  on the computational basis  $|0\rangle_n$ , and  $\mathcal{O}$  is a target Hermitian operator with eigenvalues  $\pm 1$ . We use the modified maximum likelihood estimation method based on the specific quantum circuits with the amplitude amplification operator  $Q$  and the two POVMs  $M^{(\text{even})}$ ,  $M^{(\text{odd})}$ . The measurement based on the two types of POVM yields probability distributions with different symmetries, and as a result the algorithm can estimate the mean value  $\langle A | \mathcal{O} | A \rangle$  correctly including its sign. We assume that the depolarization noise is induced when preparing  $|A\rangle$  and querying  $Q$ . Even under this noisy condition, the algorithm can estimate the target value efficiently in the sense of the Fisher information by optimizing the number of querying  $Q$  (i.e.,  $m$ ) and the type of POVM (i.e., even or odd), which are encoded together into a 1-dimensional discrete parameter  $\alpha$ . That is, the optimization improves the classical Fisher information so that it gets sufficiently close to the quantum Fisher information, when the system dimension  $d = 2^n$  is enough large.

an irrational number and also appropriately choosing  $D_k$ , Theorem 1 guarantees that there exists an  $\alpha$  such that  $\kappa$  is arbitrarily close to 1. This seems to be desirable, but we encounter the following issue. That is, if  $\kappa \rightarrow 1$ , the probability  $1 - \mathbf{P}_{\mathcal{D}}(\alpha; \theta^*)$  goes to zero, meaning that we need a large number of shots  $N$  to have a good estimate. To circumvent this issue, which can also be understood in the discontinuity of the even classical Fisher information in  $d \rightarrow \infty$  (See Appendix B or Eq. (18) with  $\kappa = 1$ ), we introduce a regularization function  $\text{Reg}(\alpha; \hat{\theta}_k)$  such that  $\text{Reg} \simeq 0$  at  $\kappa \simeq 1$  and take the objective function  $\kappa \times \text{Reg}$  rather than  $\kappa$ . Then,  $\kappa \times \text{Reg}$  is not maximized at an  $\alpha$  such that  $\kappa$  is too close to 1. But we want  $\kappa$  to be enough close to 1, hence the regularization term  $\text{Reg}$  should satisfy  $\text{Reg} \simeq 0$  only in the narrow region of  $\alpha$  satisfying  $\kappa \simeq 1$ . We employ the following regularization function satisfying this requirement:

$$\text{Reg}(\alpha; \hat{\theta}_k) := \frac{\sin^2(\alpha \hat{\theta}_k)}{1 - \delta \cos^2(\alpha \hat{\theta}_k)}. \quad (28)$$

Actually, when we employ the parameter  $\delta$  closer to 1, the regularization function becomes sharper around  $\alpha$  such that  $\kappa \simeq 1$ . Hence, we arrive at the objective function given in Eq. (27). In the numerical simulation shown later, we choose  $\delta = 0.95$ .

The optimized  $\alpha_{k+1}$  maximizes the ratio of Fisher information modified by the regularization in the finite range  $D_k$ , and thus we can employ the nearly optimal

measurement in the next  $(k+1)$ -th step. Especially, when  $\theta^*/2\pi$  is an irrational number, the existence of optimal  $\alpha_{k+1}$  is guaranteed by Theorem 1, if we choose an appropriate range  $D_k$  in the limit  $d \rightarrow \infty$ . Note that the odd  $\alpha$  also takes an important role at the beginning of the procedure, because the odd classical Fisher information is comparable to the quantum Fisher information when  $\alpha_{k+1}$  takes a relatively small value. Also, it is obvious that the optimization does not yield an amplified level such that  $\sin(\alpha \hat{\theta}_k) \simeq 0$ , and thus our method can avoid vanishing classical Fisher information regardless of the target value, which is demonstrated in the next section.

Lastly, the optimization takes a role of not only selecting an optimal  $\alpha$  to approach the quantum Fisher information, but also controlling the following trade-off by setting the optimization range of each  $\alpha_{k+1}$ . That is, a large  $\alpha$  is preferred to enhance the Fisher information per shot, but if  $\alpha$  dramatically (e.g., super-exponentially) increases with respect to  $k$ , then the estimation will be failed for a practical  $N$  because the likelihood function  $\mathcal{L}_k(\theta; \mathbf{x}_k)$  has many peaks around the true target value.

### C. Statistical properties of the estimator

Although the random variables  $X^{(k)}$  describing the measurement results depend on each other and have the hierarchical structure as shown in Eq. (26), we can prove the following desirable statistical property of the estimator; i.e., the consistency.

**Theorem 2.** (Consistency; informal version.) *There exists a unique maximum likelihood estimator  $\hat{\theta}_M$  of  $\mathcal{L}_M(\theta; \mathbf{X}_M)$  such that*

$$\cos \hat{\theta}_M \rightarrow \langle \mathcal{O} \rangle, \quad (29)$$

where  $\rightarrow$  means the convergence in probability as  $N \rightarrow \infty$ . In addition, the random variable  $\alpha_k(\mathbf{X}_{k-1})$  converges to a constant  $\alpha_k^*$  in the sense of probability as follows

$$\lim_{N \rightarrow \infty} P[\alpha_k(\mathbf{X}_{k-1}) = \alpha_k^*] = 1, \quad k = 2, \dots, M, \quad (30)$$

where  $\alpha_k(\mathbf{x}_{k-1})$  is the optimized amplified level based on the measurement results  $\mathbf{x}_{k-1}$ ; that is,  $\{\alpha_k\}$  become independent with each other, as  $N \rightarrow \infty$ .

The proof is given in Appendix D, where  $\alpha_k^*$  is given in Eq. (C.5). Theorem 2 means that the proposed estimator is valid in the sense that more data leads to more accurate estimation. That is, unlike the previous method [18] which uses Bayesian inference based on the measurement with the odd POVM (20) (not the even POVM), the estimate approaches the true value with high probability as the number of measurements  $N$  increases, as implied by Eq. (29). Note that the Bayesian inference may return estimates far from the true value as discussed in [19].

Furthermore, the asymptotic variance of the estimator can achieve the Cramér-Rao lower bound when  $N$  is large. To show this result, we focus on the following total classical/quantum Fisher information:

$$\mathcal{I}_{c,\text{tot}}(\theta^*) = N \sum_{m=1}^M \mathbf{E}_{\mathbf{X}_{m-1}} [\mathcal{I}_c(\alpha_m(\mathbf{X}_{m-1}); \theta^*)], \quad (31)$$

$$\mathcal{I}_{q,\text{tot}}(\theta^*) = N \sum_{m=1}^M \mathbf{E}_{\mathbf{X}_{m-1}} [\mathcal{I}_q(\alpha_m(\mathbf{X}_{m-1}))]. \quad (32)$$

The derivation is provided in Appendix C. Since Theorem 2 states that  $\alpha_m(\mathbf{X}_{m-1})$  converges to a constant  $\alpha_m^*$  with high probability as  $N$  increases, the total Fisher information also converges as follows;

$$\frac{\mathcal{I}_{c/q,\text{tot}}(\theta^*)}{N} \rightarrow \frac{\mathcal{I}_{c/q,\text{tot}}^*(\theta^*)}{N}, \quad (33)$$

where  $\mathcal{I}_{c/q,\text{tot}}^*(\theta^*)$  is the asymptotic value of the total classical/quantum Fisher information defined as

$$\mathcal{I}_{c,\text{tot}}^*(\theta^*) := N \sum_{m=1}^M \mathcal{I}_c(\alpha_m^*; \theta^*), \quad (34)$$

$$\mathcal{I}_{q,\text{tot}}^*(\theta^*) := N \sum_{m=1}^M \mathcal{I}_q(\alpha_m^*). \quad (35)$$

Note that  $\alpha_m^*$  depends on the target value  $\theta^*$  implicitly as in Eq. (C.5). Here, we provide the convergence theorem for the distribution of our estimator.

**Theorem 3.** (Asymptotic normality; informal version.) *If  $\hat{\theta}_M$  is a maximum likelihood estimator of  $\mathcal{L}_M(\theta; \mathbf{X}_M)$ , then the following convergence holds;*

$$\sqrt{\mathcal{I}_{c,\text{tot}}^*(\arccos \langle \mathcal{O} \rangle)} (\cos \hat{\theta}_M - \langle \mathcal{O} \rangle) \rightarrow \mathcal{N}(0, 1 - \langle \mathcal{O} \rangle^2), \quad (36)$$

where  $\mathcal{N}(0, 1 - \langle \mathcal{O} \rangle^2)$  denotes a centered normal distribution with variance  $1 - \langle \mathcal{O} \rangle^2$ , and  $\rightarrow$  means the convergence in distribution as  $N$  increases.

This theorem shows that the distribution of the estimator  $\cos \hat{\theta}_M$  gets arbitrarily close to the normal distribution with mean  $\langle \mathcal{O} \rangle$  in large  $N$ . In addition, the asymptotic variance of the estimator is proportional to the inverse of the asymptotic value of the total classical Fisher information. Thus, our estimator can asymptotically achieve the classical Cramér-Rao lower bound. In the next section, we numerically demonstrate how fast the above two asymptotic properties behave with respect to  $N$ .

Moreover, the adaptive optimization (27) yields nearly the optimal measurement at each step, and as a result the total classical Fisher information is likely sufficiently close to the total quantum Fisher information, as the number of qubits increases;

$$\mathcal{I}_{c,\text{tot}}^*(\theta^*) \approx \mathcal{I}_{q,\text{tot}}^*(\theta^*), \quad (37)$$

where the approximation error in Eq. (37) depends on the selection of the set of optimization ranges  $\{D_k\}_{k=1}^{M-1}$  and the regularization parameter  $\delta$ . In the next section, we demonstrate that the approximation error is sufficiently small for *almost all*  $\theta^*$ , via an appropriate choice of  $\{D_k\}_{k=1}^{M-1}$ ; that is, together with the asymptotic normality, our estimator achieves nearly the ultimate precision given by the inverse of total quantum Fisher information.

## IV. NUMERICAL EXPERIMENT

In this section, we numerically verify the performance of the proposed algorithm. First, in the practical (i.e., a few hundred of) measurement number  $N$ , we demonstrate that the asymptotic properties given by Theorems 2 and 3 hold. Next, by evaluating the asymptotic value of the total Fisher information, we confirm that the proposed algorithm retains a large Fisher information regardless of the target value  $\theta^*$ . We also show that the total classical Fisher information becomes sufficiently close to the quantum Fisher information for a system of dozens of qubits.

### A. Asymptotic properties with respect to the number of measurement

To demonstrate the properties of our algorithm, we numerically evaluate the root mean squared error (RMSE)

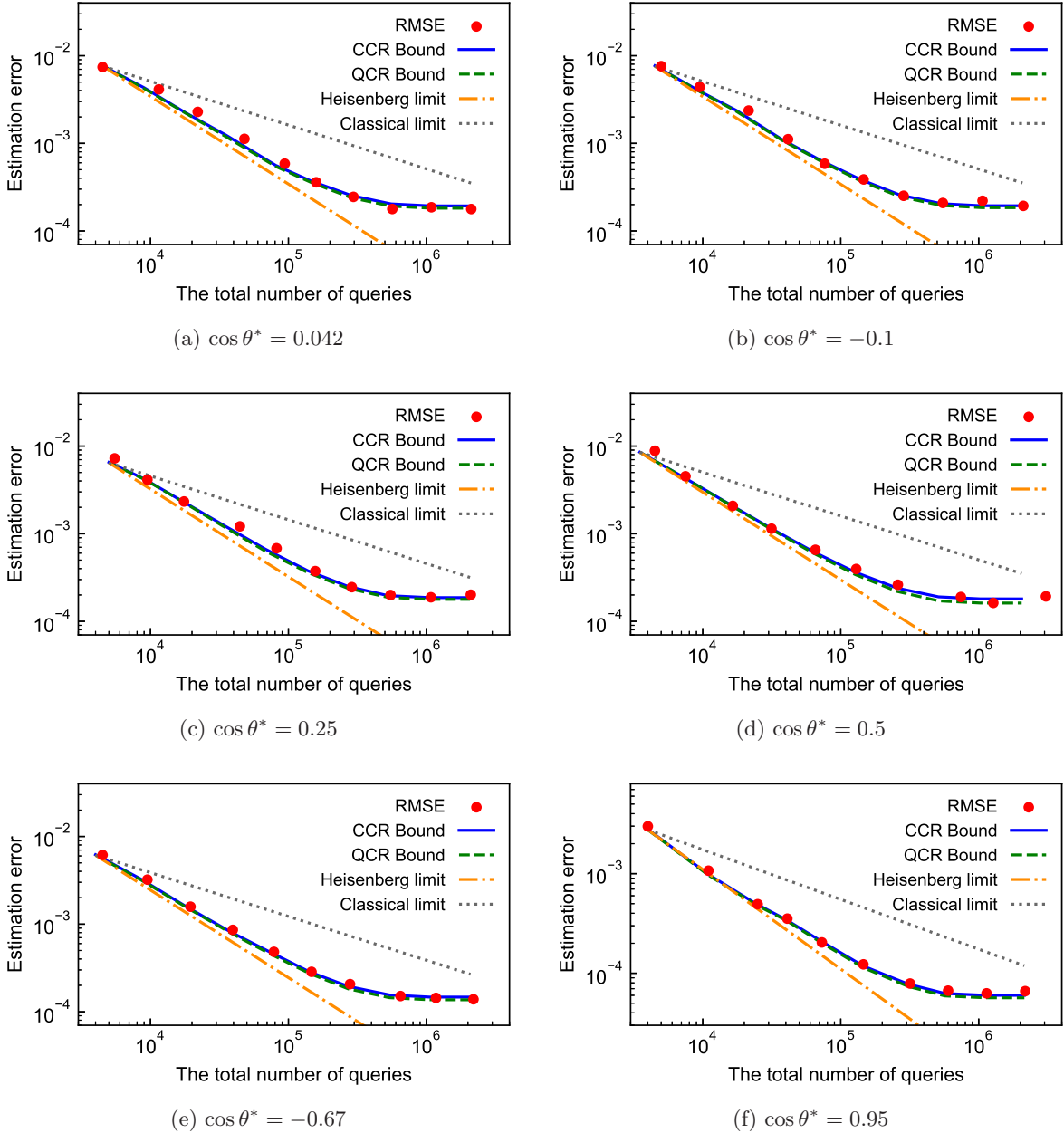


FIG. 2. The estimation error of  $\langle \mathcal{O} \rangle = \cos \theta^*$  and the total number of queries for several target values (a)–(f). The root mean squared error (RMSE) of the estimator  $\hat{\cos \theta}$  is evaluated using 200 trials. Since  $N_q$  defined in Eq. (40) is a random variable in our method, the RMSE is plotted as a function of the maximum value of  $N_q$  in 200 trials. The blue solid and green dashed lines represent the asymptotic values of CCR/QCR bounds obtained from the corresponding classical/quantum Fisher information  $\mathcal{I}_{c/q,tot}^*(\theta^*)$ , respectively. The orange dash-dotted and gray dotted lines represent the Heisenberg limit and the classical limit, respectively.

of  $\hat{\cos \theta}$  defined as

$$\begin{aligned} \text{RMSE} [\cos \hat{\theta}] &:= \sqrt{\mathbf{E}_{\hat{\theta}} \left[ \left( \cos \hat{\theta} - \cos \theta^* \right)^2 \right]} \\ &\simeq \sqrt{\frac{1}{\#} \sum_{i=1}^{\#} \left( \cos \hat{\theta}[i] - \cos \theta^* \right)^2}, \quad (38) \end{aligned}$$

where  $\#$  is the total number of trials, and  $\hat{\theta}[i]$  denotes the estimate of  $i$ th trial. In the following, we use  $\# = 200$  samples to evaluate the RMSE. We assume the depolarization noise with the parameters  $p_s = 1$  and  $p_q = 0.99$ . The number of qubits is set to 20, which corresponds to the system dimension  $d = 2^{20}$ . We also set the number of measurements as  $N = 500$  for each circuit. To ob-

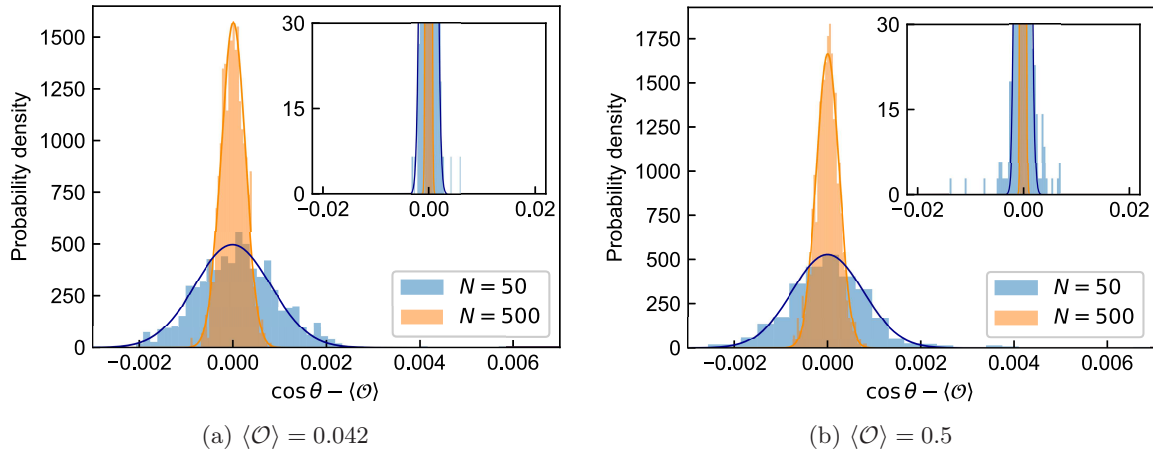


FIG. 3. The probability density of the maximum likelihood estimator  $\cos \hat{\theta}_M$  in the case of  $M = 9$ . The blue and orange plots correspond to the results with  $N = 50$  and  $N = 500$ , respectively. The histograms represent the empirical probability density over 1000 trials, and the solid lines denote the probability density of the centered normal distribution with the variance corresponding to the asymptotic CCR bound. The upper right panels show the same plots with much wider range in the horizontal axis to show the existence of outliers. The larger  $N$  becomes, the sharper the density gets around the target value, which demonstrates the consistency in Theorem 2. Also, the outliers vanish in large  $N$ ; thus the empirical density is nearly identical to the normal distribution, which is exactly the asymptotic normality in Theorem 3.

tain the maximum likelihood estimates, we used a modified brute force method, in which the search domain becomes narrowed as the measurement process proceeds. The amplified level  $\alpha_k$  of the  $k$ th measurement process ( $k = 2, \dots, M$ ) is determined by solving the optimization problem (27), where the maximum likelihood estimate  $\hat{\theta}_{k-1}$  has been obtained at the  $(k-1)$ th step. Also, in this work, the optimization range is chosen as

$$D_{k-1} := \{2^{k-1}, 2^{k-1} + 1, \dots, 2^k\}. \quad (39)$$

The exponential increase of the number of elements in  $D_{k-1}$  is inspired by the fact that, when there is no noise, the exponential increment sequence  $m_k = 2^{k-1}$  achieves the Heisenberg limit [47]; also see the discussion below Eq. (6). If there exist several  $\alpha \in D_{k-1}$  that take similar values with respect to the ratio of Fisher information, we take the smallest  $\alpha$ .

Figure 2 shows the relationship between the RMSE Eq. (38) and the total number of queries  $N_q$  defined by

$$N_q := N \sum_{k=1}^M \alpha_k. \quad (40)$$

The red plots indicate the RMSE with  $M = 3, 4, \dots, 12$  from left to right in each panel. Since  $N_q$  is a random variable due to the randomness of  $\alpha_k$ , we plot the RMSE as a function of the maximum value of  $N_q$  in  $\# = 200$  trials, and thus the RMSE plots are overestimated with respect to the number of queries. In addition, the classical Cramér-Rao (CCR) lower bound and the quantum Cramér-Rao (QCR) lower bound are depicted with the solid blue and dashed green lines, respectively; these are calculated by substituting the true value  $\theta^*$

and the asymptotic sequence  $\{\alpha_k^*\}_{k=1}^M$  into  $\mathcal{I}_{c/q,tot}^*(\theta^*)$  in Eqs. (34) and (35). Note that the difference between the bounds obtained from the  $\# = 200$  average of the total Fisher information (not shown in the figure),  $\mathcal{I}_{c/q,tot}(\theta^*)$ , and the asymptotic CCR/QCR bounds from  $\mathcal{I}_{c/q,tot}^*(\theta^*)$  can be negligible, which clearly supports Eq. (33). The orange dash-dotted and gray dotted lines represent the Heisenberg limit  $\text{RMSE} = O(1/N_q)$  and the classical (i.e., the case where no amplitude amplification operator is applied) limit  $\text{RMSE} = O(1/\sqrt{N_q})$ , respectively.

Several important features are observed. First, the CCR and QCR bounds are close to each other as expected from Eq. (37). Note that this good approximation holds even when the target value  $\theta^*/2\pi$  is a rational number as shown in the panel (d); actually, we will see in the next subsection that this approximation (37) holds for almost all  $\theta^*$  in the numerical simulation. We then find that the RMSE almost achieves the CCR and accordingly QCR bounds in all the cases of six target values (more precisely, the ratio of the RMSE to the CCR bound is at most 1.1). That is,  $N = 500$  is sufficient to obtain the asymptotic normality (36) in the chosen noise condition. Moreover, the empirical probability density of our estimator shown in Fig. 3 converges to the normal distribution whose variance corresponds to the asymptotic CCR bound as  $N$  increases, which directly demonstrates the asymptotic normality (36). Recall that this key property holds because the amplified levels are almost identical to  $\{\alpha_k^*\}_{k=1}^M$  due to Theorem 2, which is demonstrated in Fig. 6 in Appendix D.

Next, let us see the impact of noise on the performance. As  $N_q$  increases, the CCR/QCR bounds as well as RMSE become saturated around  $M = 10$ , which corresponds to

$\sim 5 \times 10^5$  in the horizontal axis in Fig. 2. This implies that the Fisher information in the case  $M > 10$  is overwhelmed by the depolarization noise. However, the RMSE decreases nearly according to the Heisenberg scaling until  $N_q \sim 10^5$ . This scaling is attributed to the quadratic speedup by the amplitude amplification, and the speedup is dominant until the amplified level reach the balancing point  $\alpha_B$  between the quadratic enhancement  $\alpha^2$  and the exponential quantum information loss  $p_q^{\alpha/2}$  in the quantum Fisher information  $\mathcal{I}_q(\alpha)$  given in Eq. (24);  $\alpha_B$  is the point maximizing  $\mathcal{I}_q(\alpha)$  as a function of  $\alpha$  and is thus given by

$$\alpha_B = \frac{4}{\log(1/p_q)}. \quad (41)$$

We can use  $\alpha_B$  to specify the lower limit of the estimation error  $\varepsilon_{\text{lim}}$  such that our algorithm can reach nearly according to the Heisenberg scaling. That is, if we choose  $M$  as the floor function  $\text{floor}(\log_2 \alpha_B)$  such that the possible maximum  $\alpha_M$  (i.e.,  $2^M$ ) takes the similar value of  $\alpha_B$ , then we can neglect the quantum information loss term approximately, and the total quantum Fisher information scales as  $\mathcal{I}_{q,\text{tot}}^*(\theta^*) = O(N\alpha_B^2)$ ; therefore, we can establish

$$\frac{1}{\varepsilon_{\text{lim}}} = O\left(\frac{\sqrt{N}}{\log(1/p_q)}\right). \quad (42)$$

Note that the number of measurements  $N$  for each circuit is fixed in this paper. In Fig. 2, even at around the saturated point in  $N_q$ , the RMSE is still in the regime that enjoys the quantum advantage below the classical limit. Thus, a simple strategy to maintain the quantum advantage in noisy environment is to fix the amplified level  $\alpha_k$  to  $\text{floor}(\alpha_B)$  when it exceeds the balancing point; then the estimator turns to be the standard maximum likelihood estimator and the RMSE decreases according to the classical scaling.

Finally, Appendix E provides the case of  $p_s = 1$  and  $p_q = 0.90$ ; that is, 10% depolarization noise is added through each operation  $Q$ , while Fig. 2 studies the case of only 1% noise. Figure 7 shows that, as expected, the quantum advantage with respect to  $N_q$  immediately vanishes.

## B. Efficiency of the estimator

As described in Section III, the classical Fisher information (23) vanishes at certain points of the amplified level  $\alpha$ . Here we show that, in the same numerical experiment as before, our algorithm can avoid those points thanks to the optimization of  $\alpha$  and as a result Eq. (37) holds for almost all  $\theta^*$ . This means that, together with the asymptotic normality (36), our estimator achieves nearly the ultimate precision. For this purpose, we calculate the asymptotic total Fisher information  $\mathcal{I}_{c/q,\text{tot}}^*(\theta^*)$

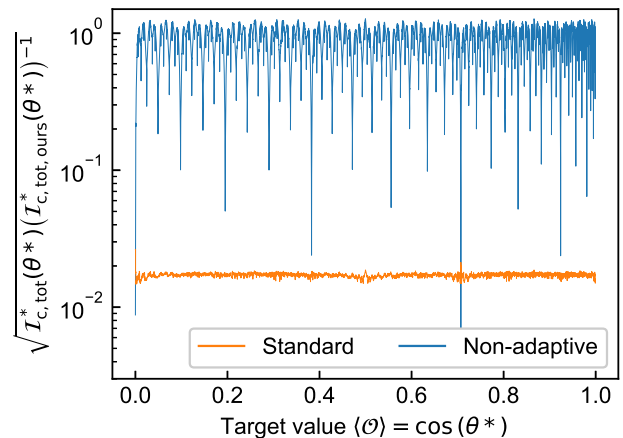


FIG. 4. Comparison of the total asymptotic classical Fisher information of our method,  $\mathcal{I}_{c,\text{tot,ours}}^*(\theta^*)$ , and the total classical Fisher information of other methods. Orange (bottom) and blue (top) lines represent the ratio of the Fisher information corresponding to the standard classical sampling method  $\alpha_k^* = 1$  and the non-adaptive method with the predefined sequence  $\alpha_1^* = 1$ ,  $\alpha_k^* = 2^k$  ( $k \geq 2$ ), respectively. The Fisher information of the standard sampling method takes a constant value 4500; thus the orange line (with rescaling in the vertical axis by the multiplication  $1/\sqrt{4500} \approx 0.015$ ) represents the estimation error of our method, showing that our adaptive method avoids singular amplified levels while the non-adaptive one suffers from this issue.

with equally distributed  $10^5$  points of  $\cos \theta^*$  in  $(0, 1)$ . The number of measurement processes is chosen as  $M = 9$ ; in this case  $D_{M-1}$  contains the balancing point  $\alpha_B$  under the chosen noise level.

Figure 4 shows the target-value dependency of the ratio between the asymptotic total classical Fisher information of our method and that of the following two methods. That is, the classical Fisher information for the standard (i.e., no amplitude amplification) sampling method, which is usually employed for VQE [2] calculations, is defined by Eq. (34) with  $\alpha_k^* = 1 \forall k$ . Also, the classical Fisher information of the method [47, 52, 53], which uses amplitude amplification yet in a non-adaptive way, is defined by Eq. (34) with  $\alpha_1^* = 1$ ,  $\alpha_k^* = 2^k \forall k \geq 2$ , where the corresponding measurement is the even POVM (14).

First note that the classical Fisher information for the standard sampling is constant regardless of the target value in the current setting; actually,  $p_s = 1$  and  $\alpha_k^* = 1 \forall k$  erases the  $\theta^*$ -dependency in the numerator and denominator in Eq. (23). Hence, the orange (bottom) line reflects that our classical Fisher information does not almost depend on the target value, meaning the robustness of the estimator. In addition, compared to the standard method, we observe the improvement of about two order of magnitude for all target values in our Fisher information. The improvement depends on the noise level, and therefore the estimation efficiency is further accelerated if the noise becomes smaller.

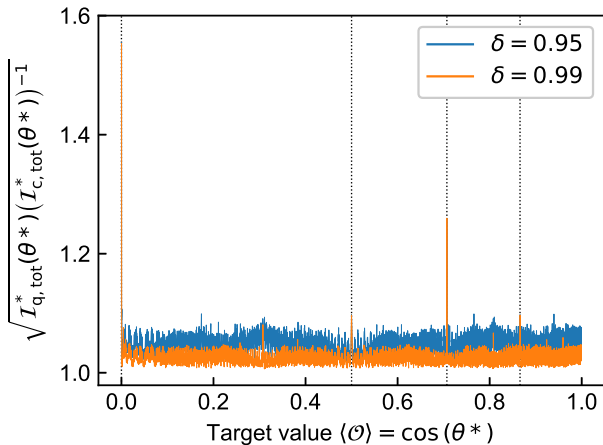


FIG. 5. Comparison of the asymptotic total classical and quantum Fisher information of our method in the case of 20-qubit system. Blue (top) and orange (bottom) lines represent the results with the regularization parameter  $\delta = 0.95$  and  $\delta = 0.99$ , respectively. The vertical dotted lines represent the target values corresponding to  $\theta^* = \pi/j$ ,  $j = 2, 3, 4, 6$  from left to right.

In contrast to our total classical Fisher information, the performance of non-adaptive method depicted with the blue (top) line heavily depends on the target value. Note that, since the total number of queries in the non-adaptive method is bigger than that in our method, there exist some target values  $\cos \theta^*$  such that the total Fisher information of ours is less than that of non-adaptive method. On the other hand, there are some target values for which the estimation error bound deviates by about two order of magnitude from ours. Therefore, when the amplified level  $\{\alpha_k\}_{k=1}^M$  is chosen non-adaptively, even if the asymptotic properties of maximum likelihood estimators hold, the estimation efficiency significantly decreases.

Finally, Fig. 5 shows the ratio of the asymptotic total classical and quantum Fisher information in our method. For almost all target values, the ratio is sufficiently close to 1, which is in line with the results discussed in the previous subsection. Moreover, as expected from the objective function in Eq. (27), relaxing the regularization as  $\delta \rightarrow 1$ , the ratio gets closer to 1, meaning that Eq. (37) holds. Recall now that, in general, the QCR bound (i.e., the ultimate limit of the estimation precision) can only be achieved when using the optimal measurement tailored for a given quantum state. Therefore, the result obtained here means that our estimation method selects the almost optimal measurements (or POVM) in the sense of Fisher information.

For the target values  $\theta^* = \pi/2, \pi/3, \pi/4, \pi/6$ , the difference of the QCR bound and the CCR bound is larger than that for other target values. This is because the values of  $(m+1)\theta^* \pmod{2\pi}$  obtained from the amplitude amplification are limited when  $\theta^*/2\pi$  is a rational num-

ber. In this case,  $(m+1)\theta^* \pmod{2\pi}$  cannot arbitrarily get close to  $\pi/2$  or  $3\pi/2$ , meaning that the classical Fisher information cannot arbitrarily get close to the quantum Fisher information; see Theorem 1 or Appendix B. The peaks at these rational points in Fig. 5 are very sharp, because the values of  $(m+1)\theta^* \pmod{2\pi}$  fill the domain  $[0, 2\pi)$  exponentially fast in the optimization of amplified levels with the chosen  $\{D_k\}_{k=1}^{M-1}$ , when the target values shift slightly from these points. Thus, these anomalous cases can be ignored in practice.

## V. CONCLUSIONS

We have proposed a quantum-enhanced mean value estimation method in a noisy environment (assumed to be the depolarization noise) that achieves the ultimate precision characterized by the quantum Fisher information under a modest number of qubits. This method employs a modified maximum likelihood estimation consisting of the amplitude amplification and the adaptive measurement; the latter is derived from the ideal POVM achieving the quantum Fisher information, and notably, it can be implemented on standard quantum computing devices. The measurement and the number of queries of the amplitude amplification operators are adaptively optimized for enhancing the classical Fisher information toward achieving the quantum Fisher information. Importantly, thanks to the maximum likelihood formulation and the two types of measurements with different symmetry in the probability distribution, our estimator enjoys some provable statistical properties such as consistency and asymptotic normality. The importance of implementable and general adaptive measurement scheme that achieves the ultimate estimation bound can also be particularly emphasized, because the actual form of such measurement is usually veiled.

To show the effectiveness of the proposed estimator, we executed several numerical experiments. The asymptotic statistical properties are evaluated in terms of the root mean squared error (RMSE), for several target values; the result was that, in all cases, the RMSE saturates the asymptotic classical and quantum Cramér-Rao lower bound, with a modest number of measurements. In particular, we confirmed that the classical Fisher information almost saturates the ultimate quantum Fisher information in a large system dimension  $d = 2^{20}$  (corresponding to a twenty-qubit system). In addition, we studied how the total Fisher information depends on the target value by evaluating the asymptotic classical/quantum Cramér-Rao lower bounds. Although the previous researches [18, 52] imply that the classical Fisher information significantly deteriorates for certain target values under depolarization noise, the proposed estimator retains a large Fisher information regardless of the target value, due to the adaptive optimization.

We believe that the estimation method presented in this paper paves the way for an interdisciplinary research

in quantum computing and quantum sensing; actually a few such trials have been found in the literature [62, 63]. Moreover, it may be useful in a wide field of quantum information technologies beyond the subroutine in quantum computing algorithms.

**Acknowledgements:** K.W. and K.F. thank IPA for

the support through MITOU target program. We would like to thank Dr. Yasunari Suzuki, Dr. Yuuki Tokunaga, and Dr. Tomoki Tanaka for helpful discussions. This work was supported by MEXT Quantum Leap Flagship Program Grant Number JPMXS0118067285 and JPMXS0120319794.

- 
- [1] M. Cerezo, A. Arrasmith, R. Babbush, S. C. Benjamin, S. Endo, K. Fujii, J. R. McClean, K. Mitarai, X. Yuan, L. Cincio, *et al.*, Variational quantum algorithms, *Nature Reviews Physics* **3**, 625 (2021).
- [2] A. Peruzzo, J. McClean, P. Shadbolt, M.-H. Yung, X.-Q. Zhou, P. J. Love, A. Aspuru-Guzik, and J. L. O’Brien, A variational eigenvalue solver on a photonic quantum processor, *Nature communications* **5**, 1 (2014).
- [3] A. Kandala, A. Mezzacapo, K. Temme, M. Takita, M. Brink, J. M. Chow, and J. M. Gambetta, Hardware-efficient variational quantum eigensolver for small molecules and quantum magnets, *Nature* **549**, 242 (2017).
- [4] B. Fuller, C. Hadfield, J. R. Glick, T. Imamichi, T. Itoko, R. J. Thompson, Y. Jiao, M. M. Kagele, A. W. Blom-Schieber, R. Raymond, *et al.*, Approximate solutions of combinatorial problems via quantum relaxations, *arXiv preprint arXiv:2111.03167* (2021).
- [5] Q. Gao, G. O. Jones, M. Motta, M. Sugawara, H. C. Watanabe, T. Kobayashi, E. Watanabe, Y.-y. Ohnishi, H. Nakamura, and N. Yamamoto, Applications of quantum computing for investigations of electronic transitions in phenylsulfonyl-carbazole TADF emitters, *npj Computational Materials* **7**, 1 (2021).
- [6] D. Amaro, M. Rosenkranz, N. Fitzpatrick, K. Hirano, and M. Fiorentini, A case study of variational quantum algorithms for a job shop scheduling problem, *EPJ Quantum Technology* **9**, 5 (2022).
- [7] C. Zoufal, R. V. Mishmash, N. Sharma, N. Kumar, A. Sheshadri, A. Deshmukh, N. Ibrahim, J. Gacon, and S. Woerner, Variational quantum algorithm for unconstrained black box binary optimization: Application to feature selection, *arXiv preprint arXiv:2205.03045* (2022).
- [8] Y. Li and S. C. Benjamin, Efficient variational quantum simulator incorporating active error minimization, *Physical Review X* **7**, 021050 (2017).
- [9] Y.-X. Yao, N. Gomes, F. Zhang, C.-Z. Wang, K.-M. Ho, T. Iadecola, and P. P. Orth, Adaptive variational quantum dynamics simulations, *PRX Quantum* **2**, 030307 (2021).
- [10] M. Benedetti, M. Fiorentini, and M. Lubasch, Hardware-efficient variational quantum algorithms for time evolution, *Physical Review Research* **3**, 10.1103/physrevresearch.3.033083 (2021).
- [11] K. Wada, R. Raymond, Y.-y. Ohnishi, E. Kaminishi, M. Sugawara, N. Yamamoto, and H. C. Watanabe, Simulating time evolution with fully optimized single-qubit gates on parametrized quantum circuits, *Physical Review A* **105**, 062421 (2022).
- [12] R. LaRose, A. Tikku, É. O’Neel-Judy, L. Cincio, and P. J. Coles, Variational quantum state diagonalization, *npj Quantum Information* **5**, 1 (2019).
- [13] M. Cerezo, K. Sharma, A. Arrasmith, and P. J. Coles, Variational quantum state eigensolver, *npj Quantum Information* **8**, 1 (2022).
- [14] G. Brassard, P. Hoyer, M. Mosca, and A. Tapp, Quantum amplitude amplification and estimation, *Contemporary Mathematics* **305**, 53 (2002).
- [15] E. Knill, G. Ortiz, and R. D. Somma, Optimal quantum measurements of expectation values of observables, *Physical Review A* **75**, 012328 (2007).
- [16] D. Wang, O. Higgott, and S. Brierley, Accelerated variational quantum eigensolver, *Phys. Rev. Lett.* **122**, 140504 (2019).
- [17] H.-Y. Huang, R. Kueng, and J. Preskill, Predicting many properties of a quantum system from very few measurements, *Nature Physics* **16**, 1050 (2020).
- [18] G. Wang, D. E. Koh, P. D. Johnson, and Y. Cao, Minimizing estimation runtime on noisy quantum computers, *PRX Quantum* **2**, 010346 (2021).
- [19] P. D. Johnson, A. A. Kunita, J. F. Gonthier, M. D. Radin, C. Buda, E. J. Doskocil, C. M. Abuan, and J. Romero, Reducing the cost of energy estimation in the variational quantum eigensolver algorithm with robust amplitude estimation, *arXiv preprint arXiv:2203.07275* (2022).
- [20] W. J. Huggins, K. Wan, J. McClean, T. E. O’Brien, N. Wiebe, and R. Babbush, Nearly optimal quantum algorithm for estimating multiple expectation values, *Phys. Rev. Lett.* **129**, 240501 (2022).
- [21] H. Cramér, *Mathematical methods of statistics* (Princeton University Press, 1946).
- [22] J. Shao, *Mathematical statistics* (Springer Science & Business Media, 2003).
- [23] A. S. Holevo, *Probabilistic and statistical aspects of quantum theory*, Vol. 1 (Springer Science & Business Media, 2011).
- [24] M. Hayashi, *Quantum information* (Springer, 2006).
- [25] C. W. Helstrom, Quantum detection and estimation theory, *Journal of Statistical Physics* **1**, 231 (1969).
- [26] C. Helstrom, The minimum variance of estimates in quantum signal detection, *IEEE Transactions on information theory* **14**, 234 (1968).
- [27] S. L. Braunstein and C. M. Caves, Statistical distance and the geometry of quantum states, *Phys. Rev. Lett.* **72**, 3439 (1994).
- [28] M. G. Paris, Quantum estimation for quantum technology, *International Journal of Quantum Information* **7**, 125 (2009).
- [29] V. Giovannetti, S. Lloyd, and L. Maccone, Advances in quantum metrology, *Nature photonics* **5**, 222 (2011).
- [30] G. Tóth and I. Apellaniz, Quantum metrology from a quantum information science perspective, *Journal of*

- Physics A: Mathematical and Theoretical **47**, 424006 (2014).
- [31] C. L. Degen, F. Reinhard, and P. Cappellaro, Quantum sensing, *Rev. Mod. Phys.* **89**, 035002 (2017).
- [32] S. Pirandola, B. R. Bardhan, T. Gehring, C. Weedbrook, and S. Lloyd, Advances in photonic quantum sensing, *Nature Photonics* **12**, 724 (2018).
- [33] P. Faist, M. P. Woods, V. V. Albert, J. M. Renes, J. Eisert, and J. Preskill, Time-energy uncertainty relation for noisy quantum metrology, in *Quantum Information and Measurement VI 2021* (Optica Publishing Group, 2021) p. W2A.3.
- [34] B. C. Sanders and G. J. Milburn, Optimal quantum measurements for phase estimation, *Phys. Rev. Lett.* **75**, 2944 (1995).
- [35] D. W. Berry and H. M. Wiseman, Optimal states and almost optimal adaptive measurements for quantum interferometry, *Phys. Rev. Lett.* **85**, 5098 (2000).
- [36] O. E. Barndorff-Nielsen and R. D. Gill, Fisher information in quantum statistics, *Journal of Physics A: Mathematical and General* **33**, 4481 (2000).
- [37] M. Hayashi, *Asymptotic Theory of Quantum Statistical Inference*, Vol. 125 (WORLD SCIENTIFIC, 2005) p. 132.
- [38] A. Fujiwara, Strong consistency and asymptotic efficiency for adaptive quantum estimation problems, *Journal of Physics A: Mathematical and General* **39**, 12489 (2006).
- [39] A. Fujiwara, Strong consistency and asymptotic efficiency for adaptive quantum estimation problems, *Journal of Physics A: Mathematical and Theoretical* **44**, 079501 (2011).
- [40] R. Demkowicz-Dobrzański, J. Kołodyński, and M. Guţă, The elusive heisenberg limit in quantum-enhanced metrology, *Nature Communications* **3**, 1063 (2012).
- [41] R. Okamoto, M. Iefuji, S. Oyama, K. Yamagata, H. Imai, A. Fujiwara, and S. Takeuchi, Experimental demonstration of adaptive quantum state estimation, *Phys. Rev. Lett.* **109**, 130404 (2012).
- [42] K. M. Svore, M. B. Hastings, and M. Freedman, Faster phase estimation, *Quantum Inf. Comput.* **14**, 306–328 (2014).
- [43] N. Wiebe and C. Granade, Efficient bayesian phase estimation, *Phys. Rev. Lett.* **117**, 010503 (2016).
- [44] T. E. O’Brien, B. Tarasinski, and B. M. Terhal, Quantum phase estimation of multiple eigenvalues for small-scale (noisy) experiments, *New Journal of Physics* **21**, 023022 (2019).
- [45] A. Dutkiewicz, B. M. Terhal, and T. E. O’Brien, Heisenberg-limited quantum phase estimation of multiple eigenvalues with few control qubits, *Quantum* **6**, 830 (2022).
- [46] I. Zintchenko and N. Wiebe, Randomized gap and amplitude estimation, *Phys. Rev. A* **93**, 062306 (2016).
- [47] Y. Suzuki, S. Uno, R. Raymond, T. Tanaka, T. Onodera, and N. Yamamoto, Amplitude estimation without phase estimation, *Quantum Information Processing* **19**, 1 (2020).
- [48] S. Aaronson and P. Rall, Quantum approximate counting, simplified, in *Symposium on Simplicity in Algorithms* (SIAM, 2020) pp. 24–32.
- [49] D. Grinko, J. Gacon, C. Zoufal, and S. Woerner, Iterative quantum amplitude estimation, *npj Quantum Information* **7**, 1 (2021).
- [50] K. Nakaji, Faster amplitude estimation, *Quantum Inf. Comput.* (2020).
- [51] E. G. Brown, O. Goktas, and W. Tham, Quantum amplitude estimation in the presence of noise, *arXiv preprint arXiv:2006.14145* (2020).
- [52] T. Tanaka, Y. Suzuki, S. Uno, R. Raymond, T. Onodera, and N. Yamamoto, Amplitude estimation via maximum likelihood on noisy quantum computer, *Quantum Information Processing* **20**, 1 (2021).
- [53] S. Uno, Y. Suzuki, K. Hisanaga, R. Raymond, T. Tanaka, T. Onodera, and N. Yamamoto, Modified grover operator for quantum amplitude estimation, *New Journal of Physics* **23**, 083031 (2021).
- [54] T. Giurgica-Tiron, I. Kerenidis, F. Labib, A. Prakash, and W. Zeng, Low depth algorithms for quantum amplitude estimation, *Quantum* **6**, 745 (2022).
- [55] T. Tanaka, S. Uno, T. Onodera, N. Yamamoto, and Y. Suzuki, Noisy quantum amplitude estimation without noise estimation, *Phys. Rev. A* **105**, 012411 (2022).
- [56] A. Callison and D. Browne, Improved maximum-likelihood quantum amplitude estimation, *arXiv preprint arXiv:2209.03321* (2022).
- [57] A. Zhao, A. Tranter, W. M. Kirby, S. F. Ung, A. Miyake, and P. J. Love, Measurement reduction in variational quantum algorithms, *Phys. Rev. A* **101**, 062322 (2020).
- [58] D. E. Koh, G. Wang, P. D. Johnson, and Y. Cao, A framework for engineering quantum likelihood functions for expectation estimation, *arXiv preprint arXiv:2006.09349* (2020).
- [59] J. M. Martyn, Z. M. Rossi, A. K. Tan, and I. L. Chuang, Grand unification of quantum algorithms, *PRX Quantum* **2**, 040203 (2021).
- [60] Z. Jiang, Quantum fisher information for states in exponential form, *Phys. Rev. A* **89**, 032128 (2014).
- [61] Y. Yao, L. Ge, X. Xiao, X. Wang, and C. P. Sun, Multiple phase estimation for arbitrary pure states under white noise, *Phys. Rev. A* **90**, 062113 (2014).
- [62] R. Demkowicz-Dobrzański and M. Markiewicz, Quantum computation speedup limits from quantum metrological precision bounds, *Phys. Rev. A* **91**, 062322 (2015).
- [63] H. Cable, M. Gu, and K. Modi, Power of one bit of quantum information in quantum metrology, *Phys. Rev. A* **93**, 040304 (2016).

## VI. APPENDIX

### A. Fisher information and Cramér-Rao inequality

Let  $\mathbf{X}$  be a multi-dimensional discrete random variable following a joint probability distribution  $\mathcal{L}(\mathbf{x}; \theta)$ , where  $\theta$  is an unknown parameter in  $\mathbb{R}$  (in our case, the domain is  $(0, \pi)$ ). Our goal is to estimate  $\theta$  or generally a function of  $\theta$ , say  $g(\theta)$  with  $g(\cdot)$  a bijective function, by constructing an estimator  $\hat{e}(\mathbf{X})$  for  $g(\theta)$ . In general, if  $\hat{e}(\mathbf{X})$  is an unbiased estimator, i.e.,  $\mathbf{E}_{\mathbf{X}}[\hat{e}(\mathbf{X})] = g(\theta)$ , then the mean squared error of  $\hat{e}(\mathbf{X})$  is bounded as

$$\text{MSE}[\hat{e}(\mathbf{X})] \geq \left( \frac{\partial g(\theta)}{\partial \theta} \right)^2 \frac{1}{\mathcal{I}_{\mathbf{c}, \text{tot}}(\theta)}. \quad (\text{A.1})$$

This is called the Cramér-Rao inequality [22]. Also,  $\mathcal{I}_{\mathbf{c}, \text{tot}}(\theta)$  is the total classical Fisher information defined

as

$$\mathcal{I}_{c,\text{tot}}(\theta) := \mathbf{E}_{\mathbf{X}} \left[ \left\{ \frac{\partial}{\partial \theta} \ln \mathcal{L}(\theta; \mathbf{X}) \right\}^2 \right]. \quad (\text{A.2})$$

For simplicity, we write  $\partial/\partial\theta$  as  $\partial_\theta$  in what follows.

Next, let us consider the estimation problem for a single parameter embedded in a quantum state  $\rho(\theta)$ . Fixing a POVM for measuring the quantum state, we can obtain the probability distribution parameterized by  $\theta$  and study Eq. (A.1). However, there is a freedom for designing a POVM in the quantum case. Utilizing this freedom, the lower bound of Eq. (A.1) can in fact be improved; that is, the following quantum Cramér-Rao inequality holds (for simplicity,  $g(\theta) = \theta$ ) [24–28]:

$$\text{MSE}[\hat{e}(\mathbf{X})] \geq \frac{1}{\mathcal{I}_c(\theta)} \geq \frac{1}{\mathcal{I}_q(\theta)}, \quad (\text{A.3})$$

where  $\mathcal{I}_c$  is the classical Fisher information associated with the probability distribution for a POVM  $\{M_k\}$  and the target state  $\rho(\theta)$ . Here,  $\mathcal{I}_q$  denotes the quantum Fisher information defined by only the quantum state  $\rho(\theta)$  as follows:

$$\mathcal{I}_q(\theta) := \text{tr} [L_{\text{SLD}}^2 \rho(\theta)], \quad (\text{A.4})$$

where  $L_{\text{SLD}}$  is the symmetric logarithmic derivative (SLD), which is defined as the Hermitian operator satisfying

$$\partial_\theta \rho(\theta) = \frac{1}{2} (L_{\text{SLD}} \rho(\theta) + \rho(\theta) L_{\text{SLD}}). \quad (\text{A.5})$$

Note that the second inequality Eq. (A.3) holds for any POVM  $\{M_k\}$  independent to  $\theta$ . Therefore, the quantum Fisher information characterizes the fundamental limit of estimation precision that cannot improve via any measurement.

## B. Analysis for the POVMs

Our problem is to estimate the target parameter  $\theta \in (0, \pi)$  embedded into the noisy quantum state

$$\rho_{\mathcal{D}}(m; \theta) = p_s p_q^m \rho(m; \theta) + \frac{1 - p_s p_q^m}{d} I_n, \quad (\text{B.1})$$

where  $\rho(m; \theta)$  is defined as Eq. (12). We additionally operate  $\mathcal{O}$  on the state (B.1) and make a measurement with the following POVM:

$$M_0 := |\bar{0}\rangle \langle \bar{0}|, \quad M_1 := |\bar{1}\rangle \langle \bar{1}|, \quad M_2 := I_n - M_0 - M_1. \quad (\text{B.2})$$

Recall that  $\mathcal{O}$  is Hermitian with eigenvalues  $\pm 1$ , and thus it is unitary; here  $\mathcal{O}$  is used to change the frequency of

trigonometric functions in  $\rho(m; \theta)$  to  $2(m+1)$ , which is the total number of querying  $A$  and  $A^\dagger$ . The POVM has the following meanings;  $M_0$  and  $M_1$  correspond to the measurement in the subspace basis  $|\bar{0}\rangle$  and  $|\bar{1}\rangle$ , respectively, and  $M_2$  corresponds to the event such that the measured state is not in the subspace  $\mathcal{S}$  given by Eq. (10).

Now, the classical Fisher information  $\mathcal{I}'_c(\theta)$  for the probability distribution

$$\{\text{tr}[M_k \mathcal{O} \rho_{\mathcal{D}}(m; \theta) \mathcal{O}]\}_{k=0}^2 \quad (\text{B.3})$$

is calculated as

$$\begin{aligned} \mathcal{I}'_c(\theta) &= 4(\eta')^2 \sin^2 [2(m+1)\theta] (m+1)^2 \\ &\times \left\{ \eta' + \frac{2(1-\eta')}{d} - \frac{d(\eta')^2 \cos^2 [2(m+1)\theta]}{d\eta' + 2(1-\eta')} \right\}^{-1} \\ &\leq \frac{4d(\eta')^2 (m+1)^2}{d\eta' + 2(1-\eta')}, \end{aligned} \quad (\text{B.4})$$

where  $\eta' := p_s p_q^{m+1/2}$  and the condition for the equality is  $\sin [2(m+1)\theta] = \pm 1$ . The most right hand side in the final line corresponds to the quantum Fisher information for the state  $\mathcal{O} \rho_{\mathcal{D}}(m; \theta) \mathcal{O}$ . Thus, for  $\theta$  satisfying the equality condition, the POVM (B.2) is optimal in the sense that the corresponding classical Fisher information gives the QCR bound. Moreover, in the limit of  $d = 2^n \rightarrow \infty$ , the classical Fisher information is equal to the quantum Fisher information except for  $(m, \theta)$  satisfying  $\sin [2(m+1)\theta] = 0$ . Note that, in general, the eigenstates of SLD operator can be used to construct the optimal measurement that exactly achieves the quantum Fisher information [27]. In our case, the POVM of optimal measurement consists of quantum states in the form of superposition of  $|\bar{0}\rangle$  and  $|\bar{1}\rangle$ , where the coefficients of the states depend on the unknown target value; the POVM (B.2) is obtained by removing this target-dependency in the coefficients.

Although the POVM (B.2) is an optimal measurement for certain  $\theta$  satisfying  $\sin [2(m+1)\theta] = \pm 1$ , its implementation is nontrivial especially for  $M_1$  because  $|\bar{1}\rangle$  is unknown. Note that the optimal POVM obtained from the SLD operator has the same difficulty in implementation. Therefore, in this paper, we focus on the 2-valued POVM (14), which can be obtained from the POVM (B.2) as follows:

$$M_0^{(\text{even})} = \mathcal{O} M_0 \mathcal{O}, \quad M_1^{(\text{even})} = \mathcal{O} (M_1 + M_2) \mathcal{O}. \quad (\text{B.5})$$

This POVM removes the element  $M_1$  from the original 3-valued POVM (B.2), meaning that the QCR bound is not achieved in general. The classical Fisher information associated with the 2-valued POVM is calculated as

$$\begin{aligned}
\mathcal{I}_c^{(\text{even})}(m; \theta) &= \frac{(2m+2)^2 \eta' \sin^2 [(m+1)\theta]}{1 - \eta' \cos^2 [(m+1)\theta] - 2 \frac{1-\eta'}{d} + \frac{1-\eta'}{\eta'} \left(1 - \frac{1-\eta'}{d}\right) \frac{1}{d \cos^2 [(m+1)\theta]}} \\
&= \frac{(2m+2)^2 \eta' \sin^2 [(m+1)\theta]}{1 - \eta' \cos^2 [(m+1)\theta]} + O\left(\frac{\tan^2 [(m+1)\theta]}{d}\right) \\
&= \mathcal{I}_q^{(\text{even})}(m) \frac{\left(1 + 2 \frac{1-\eta'}{d\eta'}\right) \sin^2 [(m+1)\theta]}{1 - \eta' \cos^2 [(m+1)\theta]} + O\left(\frac{\tan^2 [(m+1)\theta]}{d}\right) \\
&= \mathcal{I}_q^{(\text{even})}(m) \frac{\sin^2 [(m+1)\theta]}{1 - \eta' \cos^2 [(m+1)\theta]} + O\left(\frac{1}{d \cos^2 [(m+1)\theta]}\right), \tag{B.6}
\end{aligned}$$

where we assumed  $\cos [(m+1)\theta] \neq 0$  to avoid vanishing of the classical Fisher information. Here, we define the coefficient of  $\mathcal{I}_q^{(\text{even})}(m)$  in the final line as  $\kappa$ :

$$\kappa = \frac{\sin^2 [(m+1)\theta]}{1 - \eta' \cos^2 [(m+1)\theta]} \in [0, 1). \tag{B.7}$$

Then, Eq. (B.6) is expressed as

$$\mathcal{I}_c^{(\text{even})}(m; \theta) = \kappa \mathcal{I}_q^{(\text{even})}(m) + O\left(\frac{1}{d(1-\kappa)}\right). \tag{B.8}$$

Now, when  $\theta/2\pi$  is an irrational number, the set of complex numbers  $\{e^{i(m+1)\theta}\}_{m=0,1,\dots}$  with sufficiently large  $m$  fill the unit circle in the complex plane. Thus, there exists an  $m$  such that  $\cos [(m+1)\theta]$  is arbitrarily close to 0 and accordingly  $\kappa$  is arbitrarily close to 1. Therefore, from Eq. (B.8), the classical Fisher information sufficiently approaches the quantum Fisher information, under certain condition on  $(m, \theta)$ ; moreover, taking an appropriate  $m$ , we can make the convergence exponentially fast with respect to the number of qubits (recall  $d = 2^n$  with  $n$  the number of qubits). This establishes Theorem 1.

Here we point out that there is discontinuity in the classical Fisher information, which implies the instability of estimation. For this purpose, let us see the Fisher information in the limit  $d \rightarrow \infty$ :

$$\begin{aligned}
&\lim_{d \rightarrow \infty} \mathcal{I}_c^{(\text{even})}(m; \theta) \\
&= \begin{cases} 0, & \cos [(m+1)\theta] = 0 \\ \frac{4\eta'(m+1)^2 \sin^2 [(m+1)\theta]}{1 - \eta' \cos^2 [(m+1)\theta]}, & \cos [(m+1)\theta] \neq 0 \end{cases}. \tag{B.9}
\end{aligned}$$

Note that, for  $\cos [(m+1)\theta] \neq 0$ , we obtain

$$\lim_{d \rightarrow \infty} \mathcal{I}_c^{(\text{even})}(m; \theta) \leq 4\eta'(m+1)^2 = \lim_{d \rightarrow \infty} \mathcal{I}_q^{(\text{even})}(m). \tag{B.10}$$

The first equality holds for  $\cos [(m+1)\theta] = 0$  even though  $\mathcal{I}_c^{(\text{even})}(m; \theta)$  vanishes at the point as shown in Eq. (B.9). Therefore, the classical Fisher information is not continuous at  $\cos [(m+1)\theta] = 0$  in the limit  $d = 2^n \rightarrow \infty$ .

Finally, as for the other 2-valued POVM (20), comparing the Fisher information  $\mathcal{I}_{q/c}(\alpha; \theta)$  for  $\alpha = 2m+1$ , we can obtain the following inequality for  $d > 2$ :

$$\begin{aligned}
\mathcal{I}_c^{(\text{odd})}(m; \theta) &= \frac{(2m+1)^2 (p_s p_q^m)^2 \sin^2 [(2m+1)\theta]}{4\mathbf{P}_{\mathcal{D}}^{(\text{odd})}(m; \theta) \left(1 - \mathbf{P}_{\mathcal{D}}^{(\text{odd})}(m; \theta)\right)} \\
&= \frac{(2m+1)^2 (p_s p_q^m)^2 \sin^2 [(2m+1)\theta]}{1 - (p_s p_q^m)^2 \cos^2 [(2m+1)\theta]} \\
&\leq (2m+1)^2 (p_s p_q^m)^2 \\
&< \mathcal{I}_q^{(\text{odd})}(m). \tag{B.11}
\end{aligned}$$

Hence, unlike the even classical Fisher information, the odd classical Fisher information is always smaller than the quantum Fisher information even when the number of qubits increases.

### C. Statistical structure of the algorithm

In our model, the distribution of random variables  $\mathbf{X}_M$  has a hierarchical model as follows;

$$\mathcal{L}_M(\mathbf{x}_M; \theta) = \prod_{m=1}^M F_m\left(x^{(m)}; \alpha_m(\mathbf{x}_{m-1}), \theta\right), \tag{C.1}$$

where  $F_m$  is the probability function of Binomial distribution with success probability  $\mathbf{P}_{\mathcal{D}}(\alpha_m(\mathbf{x}_{m-1}); \theta)$ . Substituting Eq. (C.1) into Eq. (A.2), we obtain the total classical Fisher information as

$$\begin{aligned}
\mathcal{I}_{c,\text{tot}}(\theta) &= - \sum_{m=1}^M \mathbf{E}_{\mathbf{X}_m} \left[ \partial_\theta^2 \ln F_m \left( X^{(m)}; \alpha_m(\mathbf{X}_{m-1}), \theta \right) \right] \\
&= - \sum_{m=1}^M \sum_{\mathbf{x}_m=(x^{(1)}, \dots, x^{(m)})} \partial_\theta^2 \ln F_m \left( x^{(m)}; \alpha_m(\mathbf{x}_{m-1}), \theta \right) \mathcal{L}_m(\mathbf{x}_m; \theta) \\
&= - \sum_{m=1}^M \sum_{x^{(m)}} \sum_{\mathbf{x}_{m-1}=(x^{(1)}, \dots, x^{(m-1)})} \partial_\theta^2 \ln F_m \left( x^{(m)}; \alpha_m(\mathbf{x}_{m-1}), \theta \right) F_m \left( x^{(m)}; \alpha_m(\mathbf{x}_{m-1}), \theta \right) \mathcal{L}_{m-1}(\mathbf{x}_{m-1}; \theta) \\
&= - \sum_{m=1}^M \sum_{\mathbf{x}_{m-1}} \mathcal{L}_{m-1}(\mathbf{x}_{m-1}; \theta) \sum_{x^{(m)}} \partial_\theta^2 \ln F_m \left( x^{(m)}; \alpha_m(\mathbf{x}_{m-1}), \theta \right) F_m \left( x^{(m)}; \alpha_m(\mathbf{x}_{m-1}), \theta \right) \\
&= - \sum_{m=1}^M \sum_{\mathbf{x}_{m-1}} \mathcal{L}_{m-1}(\mathbf{x}_{m-1}; \theta) \mathbf{E}_{Y^{(m)}} \left[ \partial_\theta^2 \ln F_m \left( Y^{(m)}; \alpha_m(\mathbf{x}_{m-1}), \theta \right) \right], \tag{C.2}
\end{aligned}$$

where we used the conditional probability (C.1) in the third line.  $Y^{(m)}$  denotes a random variable following  $F_m(y^{(m)}; \alpha_m(\mathbf{x}_{m-1}), \theta)$ , with  $y^{(m)} \in \{0, 1, \dots, N\}$ . Note here that  $\mathbf{x}_{m-1}$  is not a random variable, but a realized value of  $\mathbf{X}_{m-1}$ . The expectation in the final line corresponds to the classical Fisher information in Eq. (23) multiplied by  $N$ . Thus, we can write the total classical Fisher information as

$$\mathcal{I}_{c,\text{tot}}(\theta) = N \sum_{m=1}^M \mathbf{E}_{\mathbf{X}_{m-1}} [\mathcal{I}_c(\alpha_m(\mathbf{X}_{m-1}); \theta)]. \tag{C.3}$$

Similarly, we define the corresponding total quantum Fisher information as

$$\mathcal{I}_{q,\text{tot}}(\theta) = N \sum_{m=1}^M \mathbf{E}_{\mathbf{X}_{m-1}} [\mathcal{I}_q(\alpha_m(\mathbf{X}_{m-1}))]. \tag{C.4}$$

As proved in the following subsection,  $\alpha_m^*(\mathbf{X}_{m-1}) = \alpha_m^*$  holds with high probability for all  $m$  as  $N$  increases, where  $\alpha_m^*$  is a solution of the following optimization problem for the target value  $\theta$  (not an estimate  $\hat{\theta}$ ):

$$\alpha_m^* := \operatorname{argmax}_{\alpha \in D_{m-1}} \frac{\mathcal{I}_c(\alpha; \theta)}{\mathcal{I}_q(\alpha)} \frac{\sin^2(\alpha\theta)}{1 - \delta \cos^2(\alpha\theta)}, \tag{C.5}$$

where we define  $\alpha_1^* = 1$ . Using Eq. (C.5), the asymptotic values of the total classical/quantum Fisher information are given by

$$\mathcal{I}_{c/q,\text{tot}}^*(\theta) := N \sum_{m=1}^M \mathcal{I}_{c/q}(\alpha_m^*; \theta). \tag{C.6}$$

Then we have

$$\lim_{N \rightarrow \infty} \frac{\mathcal{I}_{c/q,\text{tot}}(\theta)}{N} = \sum_{m=1}^M \mathcal{I}_{c/q}(\alpha_m^*; \theta) = \frac{\mathcal{I}_{c/q,\text{tot}}^*(\theta)}{N}, \tag{C.7}$$

which characterizes the variance of our estimator in the asymptotic regime.

#### D. Proof for statistical properties

Let  $\theta^* \in (0, \pi)$  satisfying  $\cos \theta^* = \langle \mathcal{O} \rangle$  be a target value to be estimated. Since the objective function in Eq. (C.5) vanishes at  $\alpha \theta^* = l\pi$  ( $l \in \mathbb{Z}$ ), then the definition of  $\alpha_m^*$  leads to  $\alpha_m^* \theta^* \neq l\pi$  for  $m = 2, 3, \dots, M$ . Thus, we can take an integer  $z_m$  satisfying

$$\theta^* \in \Theta^{(m)} := \left( \frac{z_m}{\alpha_m^*} \pi, \frac{z_m + 1}{\alpha_m^*} \pi \right), \quad \forall m, \tag{D.1}$$

and define  $\Theta_M := \bigcap_{m=1}^M \Theta^{(m)}$ .

**Theorem 2.** *There exists a unique maximum likelihood estimator  $\hat{\theta}_M$  of  $\mathcal{L}_M(\theta; \mathbf{X}_M)$  such that  $\cos \hat{\theta}_M \rightarrow \cos \theta^*$  (convergence in probability) with the probability approaching 1 as  $N \rightarrow \infty$ , and*

$$\lim_{N \rightarrow \infty} P[\alpha_k(\mathbf{X}_{k-1}) = \alpha_k^*] = 1 \tag{D.2}$$

holds for all  $k = 2, \dots, M$ .

As a demonstration of Theorem 2, we provide an example of the realized amplified levels in Fig. 6. Here, the experimental settings are equivalent to those in Section IV A. Figure 6 shows that the amplified levels converge rapidly to the asymptotic values, and therefore the total Fisher information and query complexity also show rapid convergence.

*Proof.* Let  $E(m)$  be the following event:  $\alpha_k(\mathbf{X}_{k-1}) = \alpha_k^*$  holds for all  $k = 1, 2, \dots, m$ , and there exists a unique maximum likelihood estimator  $\hat{\theta}_m$  of  $\mathcal{L}_m(\theta; \mathbf{X}_m)$  which converges to  $\theta^*$ . Note that if we establish  $\hat{\theta}_m \rightarrow \theta^*$ , then this immediately leads to  $\cos \hat{\theta}_m \rightarrow \cos \theta^*$  due to the continuous mapping theorem.

In the case of  $m = 1$ , the likelihood function  $\mathcal{L}_1(\theta; \mathbf{X}_1)$  is equivalent to  $F_1(X^{(1)}; \alpha_1^*, \theta)$ . Because the success

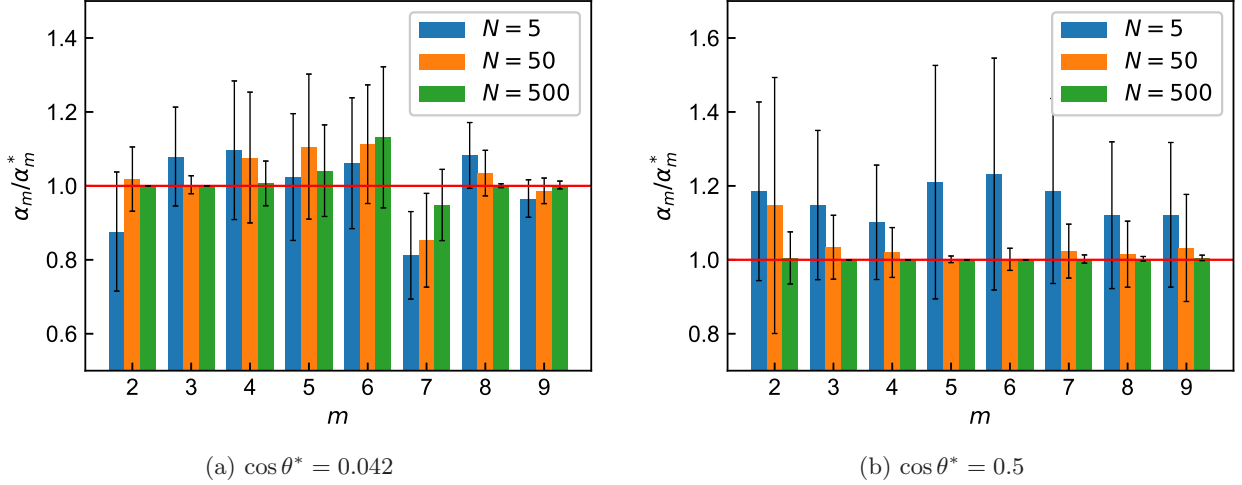


FIG. 6. Convergence of the amplified levels  $\alpha_m$ . The color bars represent the average of the realized amplified levels normalized by its asymptotic values  $\alpha_m^*$  over 1000 trials, and the error bars denote the standard deviation. With a fixed value of  $m$ , the three color bars show the results corresponding to  $N = 5$  (left, blue),  $N = 50$  (center, orange), and  $N = 500$  (right, green), respectively.

probability  $\mathbf{P}_{\mathcal{D}}(\alpha_1^*; \cdot) : (0, \pi) \rightarrow (0, 1)$  is injective and the likelihood equation

$$\partial_{\theta} \ln F_1(X^{(1)}; \alpha_1^*, \theta) = 0 \quad (\text{D.3})$$

has a unique solution when a solution exists, it follows that

$$P[E(1)] \rightarrow 1 \text{ as } N \rightarrow \infty, \quad (\text{D.4})$$

from the theory of maximum likelihood estimation [22].

Here, we assume that  $P[E(M-1)] \rightarrow 1$  for  $M \geq 2$ . For simplicity, we identify the classical Fisher information  $\mathcal{I}_c(\alpha; \theta)$  with the objective function in Eq. (27) in this proof. Fixing  $\alpha$  in the objective function  $\mathcal{I}_c(\alpha; \theta)$ , we can confirm that  $\mathcal{I}_c(\alpha; \hat{\theta}_{M-1})$  converges smoothly to  $\mathcal{I}_c(\alpha; \theta^*)$  when  $\hat{\theta}_{M-1} \rightarrow \theta^*$ . If there is a unique point maximizing  $\mathcal{I}_c(\alpha; \theta^*)$  in the range of  $D_{M-1}$ , then there exists some small number  $\epsilon' > 0$ , and the following implication holds

$$\left\{ \left| \hat{\theta}_{M-1} - \theta^* \right| < \epsilon' \right\} \subseteq \left\{ \alpha_M(\mathbf{X}_{M-1}) = \alpha_M^* \right\}, \quad (\text{D.5})$$

where  $\{\cdot\}$  denotes a set of events such as

$$\left\{ \mathbf{x}_{M-1} : \left| \hat{\theta}_{M-1}(\mathbf{x}_{M-1}) - \theta^* \right| < \epsilon' \right\}. \quad (\text{D.6})$$

Note that even if the maximum point of  $\mathcal{I}_c(\alpha; \theta^*)$  in  $D_{M-1}$  is not unique, Eq. (D.5) also holds when we adopt the minimum value in a subset  $\bar{D}_{M-1}$  of  $D_{M-1}$  as the realization of  $\alpha_M(\mathbf{X}_{M-1})$ . Here, the subset  $\bar{D}_{M-1}$  consists of elements in  $D_{M-1}$  satisfying

$$\left| \mathcal{I}_c(\alpha; \hat{\theta}_{M-1}) - \mathcal{I}_{c, M-1}^{(\max)}(\hat{\theta}_{M-1}) \right| < \epsilon_{\text{threshold}}, \quad (\text{D.7})$$

where  $\epsilon_{\text{threshold}}$  is a small positive number, and

$$\mathcal{I}_{c, M-1}^{(\max)}(\hat{\theta}_{M-1}) := \max_{\alpha \in D_{M-1}} \mathcal{I}_c(\alpha; \hat{\theta}_{M-1}). \quad (\text{D.8})$$

Note that  $\alpha_M^*$  is defined as the minimum value of  $\bar{D}_{M-1}$  for  $\theta^*$ . In the limit of  $\hat{\theta}_{M-1} \rightarrow \theta^*$ ,  $\bar{D}_{M-1}$  for  $\hat{\theta}_{M-1}$  has the same elements in  $\bar{D}_{M-1}$  for  $\theta^*$ , and therefore the implication in Eq. (D.5) holds. From the assumption  $P[E(M-1)] \rightarrow 1$ , there exists  $N_1^* \in \mathbb{N}$  for all  $\eta > 0$  such that

$$P \left[ E(M-1) \cap \left\{ \left| \hat{\theta}_{M-1} - \theta^* \right| < \epsilon' \right\} \right] > 1 - \eta \quad (\text{D.9})$$

holds for all  $N > N_1^*$ . The implication in Eq. (D.5) yields the following inequality

$$\begin{aligned} 1 - \eta &< P \left[ E(M-1) \cap \left\{ \left| \hat{\theta}_{M-1} - \theta^* \right| < \epsilon' \right\} \right] \\ &\leq P \left[ E(M-1) \cap \left\{ \alpha_M(\mathbf{X}_{M-1}) = \alpha_M^* \right\} \right] \\ &\leq P \left[ \left\{ \alpha_k(\mathbf{X}_{k-1}) = \alpha_k^* \forall k \right\} \right]. \end{aligned} \quad (\text{D.10})$$

Note that if  $\alpha_k(\mathbf{x}_{k-1}) = \alpha_k^*$  holds for all  $k = 1, 2, \dots, M$ , then the likelihood function  $\mathcal{L}_M(\theta; \mathbf{x}_M)$  can be written as

$$\begin{aligned} \mathcal{L}_M(\theta; \mathbf{x}_M) &= \prod_{m=1}^M F_m(x^{(m)}; \alpha_m(\mathbf{x}_{m-1}), \theta) \\ &= \prod_{m=1}^M F_m(x^{(m)}; \alpha_m^*, \theta). \end{aligned} \quad (\text{D.11})$$

On the other hand, Lemma 2 guarantees the existence of some natural number  $N_2^*$  such that

$$P[\mathbf{A}] > 1 - \eta, \quad (\text{D.12})$$

for all  $N > N_2^*$ , where an event  $\mathbf{A}$  is defined as

$\mathbf{A}$ :  $\prod_{m=1}^M F_m(X^{(m)}; \alpha_m^*, \theta)$  has a unique maximum

---

$$\begin{aligned}
& P[E(M)] \\
&= P\left[\left\{\mathcal{L}_M(\theta; \mathbf{X}_M) \text{ has a unique maximum point } \hat{\theta}_M \text{ such that } \hat{\theta}_M \rightarrow \theta^*\right\} \cap \left\{\alpha_k(\mathbf{X}_{k-1}) = \alpha_k^* \forall k = 1, 2, \dots, M\right\}\right] \\
&= P\left[\left\{\prod_{m=1}^M F_m(X^{(m)}; \alpha_m^*, \theta) \text{ has a unique maximum point } \hat{\theta}_M \text{ such that } \hat{\theta}_M \rightarrow \theta^*\right\} \cap \left\{\alpha_k(\mathbf{X}_{k-1}) = \alpha_k^* \forall k\right\}\right] \\
&= P\left[\mathbf{A} \cap \left\{\alpha_k(\mathbf{X}_{k-1}) = \alpha_k^* \forall k\right\}\right] > 1 - 2\eta. \tag{D.13}
\end{aligned}$$

In conclusion, we have proved that  $P[E(M)] \rightarrow 1$  also holds, and the mathematical induction establishes the theorem.  $\square$

To prove Lemma 2 or Eq. (D.12), we first establish the existence of a solution for the likelihood equation on  $F_m$ .

**Lemma 1.** *A natural number  $2 \leq m \leq M$  is fixed arbitrarily. Suppose  $P[\alpha_m(\mathbf{X}_{m-1}) = \alpha_m^*] \rightarrow 1$  as the number of measurements  $N$  increases, then  $F_m(X^{(m)}; \alpha_m^*, \theta)$  has*

---

point  $\hat{\theta}_M$  such that  $\hat{\theta}_M \rightarrow \theta^*$ .

From Eqs. (D.10) and (D.12), if we choose  $N > \max\{N_1^*, N_2^*\}$ , then

---

a unique maximum point  $\hat{\theta}^{(m)}$  in  $\Theta_m$  such that  $\hat{\theta}^{(m)} \rightarrow \theta^*$  with the probability approaching 1.

*Proof.* We first show

$$P\left[F_m(X^{(m)}; \alpha_m^*, \theta^*) > F_m(X^{(m)}; \alpha_m^*, \theta)\right] \rightarrow 1 \tag{D.14}$$

holds for any  $\theta \in \Theta_m$ ,  $\theta \neq \theta^*$ . The l.h.s can be transformed as

$$\begin{aligned}
& P\left[F_m(X^{(m)}; \alpha_m^*, \theta^*) > F_m(X^{(m)}; \alpha_m^*, \theta)\right] \\
&= \sum_{x^{(m)}} \sum_{\mathbf{x}_{m-1}} \mathcal{L}_{m-1}(\mathbf{x}_{m-1}; \theta^*) F_m(x^{(m)}; \alpha_m(\mathbf{x}_{m-1}), \theta^*) \mathbf{1}\left\{F_m(X^{(m)}; \alpha_m^*, \theta^*) > F_m(X^{(m)}; \alpha_m^*, \theta)\right\}(x^{(m)}) \\
&= \sum_{\alpha'_m \in D_{m-1}} \sum_{\substack{\mathbf{x}_{m-1}: \\ \alpha_m(\mathbf{x}_{m-1}) = \alpha'_m}} \mathcal{L}_{m-1}(\mathbf{x}_{m-1}; \theta^*) \sum_{x^{(m)}} F_m(x^{(m)}; \alpha'_m, \theta^*) \mathbf{1}\left\{F_m(X^{(m)}; \alpha_m^*, \theta^*) > F_m(X^{(m)}; \alpha_m^*, \theta)\right\}(x^{(m)}) \\
&= \sum_{\alpha'_m \in D_{m-1}} P[\alpha_m(\mathbf{X}_{m-1}) = \alpha'_m] \sum_{x^{(m)}} F_m(x^{(m)}; \alpha'_m, \theta^*) \mathbf{1}\left\{F_m(X^{(m)}; \alpha_m^*, \theta^*) > F_m(X^{(m)}; \alpha_m^*, \theta)\right\}(x^{(m)}), \tag{D.15}
\end{aligned}$$

where  $\mathbf{1}\{\cdot\}(x)$  denotes an indicator function. By assumption, the summation for  $\alpha'_m$  of the last line vanishes except for the term with  $\alpha'_m = \alpha_m^*$  as  $N$  increases. Thus, the remaining term can be written as

$$P\left[F_m(Y^{(m)}; \alpha_m^*, \theta^*) > F_m(Y^{(m)}; \alpha_m^*, \theta)\right], \tag{D.16}$$

where  $Y^{(m)}$  denotes a random variable following

$$\text{Bin}(N, \mathbf{P}_{\mathcal{D}}(\alpha_m^*; \theta^*)). \tag{D.17}$$

Since the probability  $\mathbf{P}_{\mathcal{D}}(\alpha_m^*; \theta)$  is an injective function with respect to  $\theta \in \Theta_m$ ; and its support is independent

---

to  $\theta$ , these conditions yield

$$P\left[F_m(Y^{(m)}; \alpha_m^*, \theta^*) > F_m(Y^{(m)}; \alpha_m^*, \theta)\right] \rightarrow 1, \tag{D.18}$$

as  $N \rightarrow \infty$ . We can prove this from law of large numbers for independent Bernoulli trials on  $Y^{(m)}$  and the non-negativity of the Kullback-Leibler divergence. Combining Eqs. (D.18), (D.15), we complete the proof of Eq. (D.14).

By definition of  $\Theta_m$ , we can choose a small positive number  $\delta$  such that  $(\theta^* - \delta, \theta^* + \delta) \subset \Theta_m$ . Let  $\mathbf{B}_{\pm}$  be the following events

$\mathbf{B}_{\pm}$ :  $F_m(X^{(m)}; \alpha_m^*, \theta^*) > F_m(X^{(m)}; \alpha_m^*, \theta^* \pm \delta)$  holds.

Considering  $x^{(m)} \in \mathbf{B}_+ \cap \mathbf{B}_-$ , the equation

$$\frac{\partial}{\partial \theta} F_m \left( x^{(m)}; \alpha_m^*, \theta \right) = 0, \quad (\text{D.19})$$

has solutions, and we write  $\hat{\theta}^{(m)}$  as the solution closest to  $\theta^*$  among them. Since the difference between  $\hat{\theta}^{(m)}$  and  $\theta^*$  is less than  $\delta$ ; and for all  $\epsilon > 0$  there exists  $N^* \in \mathbb{N}$  such that  $P[\mathbf{B}_\pm] > 1 - \epsilon$  for all  $N > N^*$  by Eq. (D.14), we obtain

$$P \left[ \left| \hat{\theta}^{(m)} - \theta^* \right| < \delta \right] \geq P[\mathbf{B}_+ \cap \mathbf{B}_-] > 1 - 2\epsilon. \quad (\text{D.20})$$

In addition, the likelihood equation Eq. (D.19) has a unique solution maximizing  $F_m(x^{(m)}; \alpha_m^*, \theta)$  in  $\Theta_m$  if a solution of Eq. (D.19) exists in  $\Theta_m$ . Therefore,  $\hat{\theta}^{(m)}$  is a unique maximum point of  $F_m(x^{(m)}; \alpha_m^*, \theta)$  in  $\Theta_m$ .  $\square$

Applying Lemma 1 to all the functions  $\{F_m\}$ , we establish the existence of a unique maximum point of the product function  $\Pi_m F_m$ .

**Lemma 2.** *Suppose  $P[\alpha_k(\mathbf{X}_{k-1}) = \alpha_k^*] \rightarrow 1$  for all  $k = 2, \dots, M$  and  $\hat{\theta}^{(1)} \rightarrow \theta^*$  (convergence in probability)*

---


$$P \left[ \text{there exists a maximum point } \hat{\theta}_M \text{ of } \prod_{m=1}^M F_m \left( X^{(m)}; \alpha_m^*, \theta \right) \text{ in } \Theta_M \text{ such that } \hat{\theta}_M \xrightarrow{P} \theta^* \right] \geq P[\mathbf{C}] > 1 - \epsilon, \quad (\text{D.22})$$

where we use the fact that  $\hat{\theta}_{\min}, \hat{\theta}_{\max} \rightarrow \theta^*$  yields  $\hat{\theta}_M \rightarrow \theta^*$ .

Considering the original domain of  $\theta$ , i.e.,  $(0, \pi)$ , each  $F_m$  is a periodic function and is generally maximized at multiple points. Here,  $\hat{\theta}^{(m)}$  is one of these points. However, many of these peaks are canceled out with each other by multiplication in  $\Pi_m F_m$  except for the peaks in  $\Theta_M$ . Since  $F_1$  has a unique global maximum point  $\hat{\theta}^{(1)}$ , and therefore  $\Theta_M$  is the only region where all functions  $F_m$  have a peak simultaneously as  $N$  increases. Consequently, the maximum of  $\Pi_{m=1}^M F_m(X^{(m)}; \alpha_m^*, \theta)$  in  $\Theta_M$  becomes the global maximum in  $(0, \pi)$ .  $\square$

Finally, we prove that, when  $N$  is large, the asymptotic variance of our estimator can achieve the classical Cramér-Rao lower bound.

**Theorem 3.** *If  $\hat{\theta}_M$  is a maximum likelihood estimator on  $\mathcal{L}_M(\theta; \mathbf{X}_M)$  such that  $\hat{\theta}_M \rightarrow \theta^*$  (convergence in probability), then the following convergence holds;*

$$\sqrt{\mathcal{I}_{\text{c,tot}}^*(\theta^*)} \left( \cos \hat{\theta}_M - \cos \theta^* \right) \rightarrow \mathcal{N}(0, \sin^2 \theta^*), \quad (\text{D.23})$$

*ity). Then, there exists a unique maximum point  $\hat{\theta}_M$  of the product function  $\Pi_{m=1}^M F_m(X^{(m)}; \alpha_m^*, \theta)$  in  $(0, \pi)$  such that  $\hat{\theta}_M \rightarrow \theta^*$  with the probability approaching 1 as  $N \rightarrow \infty$ .*

*Proof.* From the assumption and Lemma 1, we can choose  $N^* \in \mathbb{N}$  for all  $\epsilon > 0$  such that the probability of occurrence of the following event  $\mathbf{C}$  is bigger than  $1 - \epsilon$  for all  $N > N^*$ ;

**C:** For all  $m$ ,  $\hat{\theta}^{(m)}$  exists in  $\Theta_M$ , where  $\hat{\theta}^{(m)}$  denotes a maximum point of  $F_m(X^{(m)}; \alpha_m^*, \theta)$ .

Let  $\hat{\theta}_{\max}$  ( $\hat{\theta}_{\min}$ ) be the maximum (minimum) value of a set  $\{\hat{\theta}^{(m)}\}$ . Since the product function  $\Pi_{m=1}^M F_m$  is a continuous function with respect to  $\theta$ , it has a maximum point  $\hat{\theta}_M$  in  $[\hat{\theta}_{\min}, \hat{\theta}_{\max}]$ . Note that  $\hat{\theta}_{\max}$  and  $\hat{\theta}_{\min}$  themselves cannot be a maximum point, because the gradient at these points does not vanish, i.e.,

$$\frac{\partial}{\partial \theta} \prod_{m=1}^M F_m \left( X^{(m)}; \alpha_m^*, \theta \right) \Bigg|_{\theta=\hat{\theta}_{\max}, \hat{\theta}_{\min}} \neq 0, \quad (\text{D.21})$$

where the gradient is positive (negative) for  $\hat{\theta}_{\min}$  ( $\hat{\theta}_{\max}$ ), respectively. Therefore, we obtain

---

where  $\mathcal{N}$  denotes a centered normal distribution with variance  $\sin^2 \theta^*$  and  $\rightarrow$  means the convergence in distribution as  $N$  increases.

*Proof.* Using the Taylor's theorem, we can expand  $\partial_\theta \ln \mathcal{L}_M(\theta; \mathbf{X}_M)$  around  $\theta = \theta^*$  as

$$\begin{aligned} \partial_\theta \ln \mathcal{L}_M(\theta; \mathbf{X}_M) &= \partial_\theta \ln \mathcal{L}_M(\theta^*; \mathbf{X}_M) \\ &\quad + \partial_\theta^2 \ln \mathcal{L}_M(\theta^*; \mathbf{X}_M)(\theta - \theta^*) \\ &\quad + \frac{1}{2} \partial_\theta^3 \ln \mathcal{L}_M(\theta'; \mathbf{X}_M)(\theta - \theta^*)^2, \end{aligned} \quad (\text{D.24})$$

where  $\theta'$  denotes some real number between  $\theta$  and  $\theta^*$ . Since  $\hat{\theta}_M$  is a root of the likelihood equation, we obtain

$$\sqrt{\mathcal{I}_{\text{c,tot}}^*(\theta^*)} (\hat{\theta}_M - \theta^*) = \frac{A}{B - C}, \quad (\text{D.25})$$

where for simplicity we introduced the random variables  $A$ ,  $B$ , and  $C$  defined as

$$A := (\mathcal{I}_{\text{c,tot}}^*(\theta^*))^{-1/2} \partial_\theta \ln \mathcal{L}_M(\theta^*; \mathbf{X}_M),$$

$$B := -(\mathcal{I}_{c,\text{tot}}^*(\theta^*))^{-1} \partial_\theta^2 \ln \mathcal{L}_M(\theta^*; \mathbf{X}_M),$$

$$C := (2\mathcal{I}_{c,\text{tot}}^*(\theta^*))^{-1} \partial_\theta^3 \ln \mathcal{L}_M(\theta'; \mathbf{X}_M)(\hat{\theta}_M - \theta^*).$$

Here, we show that  $A$  converges to the standard normal distribution. To apply Lemma 3, we first calculate the characteristic function of  $A$  replacing  $\mathbf{X}_M, \alpha_m \rightarrow \mathbf{Y}_M, \alpha_m^*$ , where  $\mathbf{Y}_M = (Y^{(1)}, \dots, Y^{(M)})$  is a random vector whose element follows Binomial distribution  $\text{Bin}(N, \mathbf{P}_{\mathcal{D}}(\alpha_m^*; \theta^*))$  independently. That is, for  $t \in \mathbb{R}$  we have

$$\begin{aligned} & \mathbf{E} \left[ \exp(it A) \Big|_{\mathbf{X}_M, \alpha_m \rightarrow \mathbf{Y}_M, \alpha_m^*} \right] \\ &= \mathbf{E} \left[ \exp \left( \frac{it \sum_{m=1}^M \partial_\theta \ln F_m(Y^{(m)}; \alpha_m^*, \theta^*)}{\sqrt{\mathcal{I}_{c,\text{tot}}^*(\theta^*)}} \right) \right] \\ &= \prod_{m=1}^M \left( \mathbf{E} \left[ \exp \left( \frac{it \partial_\theta \ln f_m(Y_1^{(m)}; \alpha_m^*, \theta^*)}{\sqrt{\mathcal{I}_{c,\text{tot}}^*(\theta^*)}} \right) \right] \right)^N \\ &= \prod_{m=1}^M \left( 1 - \frac{t^2}{2N} \frac{\mathcal{I}_c(\alpha_m^*; \theta^*)}{\sum_{m=1}^M \mathcal{I}_c(\alpha_m^*; \theta^*)} + o\left(\frac{1}{N}\right) \right)^N \\ &\rightarrow \exp\left(-\frac{t^2}{2}\right), \end{aligned} \quad (\text{D.26})$$

where  $Y_1^{(m)}$  denotes a random variable following Bernoulli distribution with the success probability  $\mathbf{P}_{\mathcal{D}}(\alpha_m^*; \theta^*)$ , and  $f_m$  is the probability function of  $Y_1^{(m)}$ . Thus, Lemma 3 yields

$$\lim_{N \rightarrow \infty} \mathbf{E} [\exp(itA)] = \exp\left(-\frac{t^2}{2}\right). \quad (\text{D.27})$$

Therefore,  $A \rightarrow \mathcal{N}(0, 1)$  holds.

Next, we consider the convergence of  $B$ . According to the Chebyshev inequality, for all  $c > 0$  we obtain

$$P[|B - 1| > c] \leq \frac{\mathbf{E}[(B - 1)^2]}{c^2}. \quad (\text{D.28})$$

Here,  $(B - 1)^2$  is upper bounded, and the expectation of  $(B - 1)^2$  replacing  $\mathbf{X}_M, \alpha_m \rightarrow \mathbf{Y}_M, \alpha_m^*$  also converges to 0 as follows. For simplicity, we define  $W_m(Y^{(m)})$  and  $w_m(Y^{(m)})$  as

$$\begin{aligned} W_m(Y^{(m)}) &:= \partial_\theta^2 \ln F_m(Y^{(m)}; \alpha_m^*, \theta^*) \\ &\quad - \mathbf{E} \left[ \partial_\theta^2 \ln F_m(Y^{(m)}; \alpha_m^*, \theta^*) \right], \end{aligned}$$

$$\begin{aligned} w_m(Y_1^{(m)}) &:= \partial_\theta^2 \ln f_m(Y_1^{(m)}; \alpha_m^*, \theta^*) \\ &\quad - \mathbf{E} \left[ \partial_\theta^2 \ln f_m(Y_1^{(m)}; \alpha_m^*, \theta^*) \right], \end{aligned}$$

respectively.

$$\begin{aligned} & \mathbf{E} \left[ (B - 1)^2 \Big|_{\mathbf{X}_M, \alpha_m \rightarrow \mathbf{Y}_M, \alpha_m^*} \right] \\ &= \frac{\text{Var} \left[ \partial_\theta^2 \ln \prod_{m=1}^M F_m(Y^{(m)}; \alpha_m^*, \theta^*) \right]}{[\mathcal{I}_{c,\text{tot}}^*(\theta^*)]^2} \\ &= \frac{\sum_{n,m=1}^M \mathbf{E} [W_m(Y^{(m)}) W_n(Y^{(n)})]}{[\mathcal{I}_{c,\text{tot}}^*(\theta^*)]^2} \\ &= \frac{N}{[\mathcal{I}_{c,\text{tot}}^*(\theta^*)]^2} \sum_{m=1}^M \mathbf{E} [w_m^2(Y_1^{(m)})] \\ &= \frac{1}{N} \frac{\sum_{m=1}^M \mathbf{E} [w_m^2(Y_1^{(m)})]}{\left[ \sum_{m=1}^M \mathcal{I}_c(\alpha_m^*; \theta^*) \right]^2} \rightarrow 0, \end{aligned} \quad (\text{D.29})$$

where we used  $\mathcal{I}_{c,\text{tot}}^*(\theta^*) = -\mathbf{E}[\partial_\theta^2 \ln \prod_{m=1}^M F_m]$  for the first equality. Thus, Lemma 3 establishes that  $B \rightarrow 1$  holds.

Since  $N^{-1} \partial_\theta^3 \ln \mathcal{L}_M(\theta'; \mathbf{x}_M)$  is also upper bounded,  $\hat{\theta}_M - \theta^* \rightarrow 0$  yields  $C \rightarrow 0$ . To sum up the above asymptotic properties, we conclude that the following convergence holds;

$$\sqrt{\mathcal{I}_{c,\text{tot}}^*(\theta^*)}(\hat{\theta}_M - \theta^*) \rightarrow \mathcal{N}(0, 1). \quad (\text{D.30})$$

In addition, the delta method [22] yields a more suitable expression

$$\sqrt{\mathcal{I}_{c,\text{tot}}^*(\theta^*)}(\cos \hat{\theta}_M - \cos \theta^*) \rightarrow \mathcal{N}(0, \sin^2 \theta^*). \quad (\text{D.31})$$

□

To complete the proof of Theorem 3, we finally show the following lemma.

**Lemma 3.** *Let  $h(\mathbf{x}_M, \alpha_2, \dots, \alpha_M)$  be an upper bounded function on  $\mathbf{x}_M \in \{0, 1, \dots, N\}^M$  and  $Y^{(m)}$  ( $m = 1, 2, \dots, M$ ) be an independent random variable following Binomial distribution  $\text{Bin}(N, \mathbf{P}_{\mathcal{D}}(\alpha_m^*; \theta^*))$ . Suppose that  $\mathbf{E}[h(\mathbf{Y}_M, \alpha_2^*, \dots, \alpha_M^*)]$  converges to some constant  $\beta$  as  $N \rightarrow \infty$ , then the following convergence holds*

$$\lim_{N \rightarrow \infty} \mathbf{E} [h(\mathbf{X}_M, \alpha_2(\mathbf{X}_1), \dots, \alpha_M(\mathbf{X}_{M-1}))] = \beta. \quad (\text{D.32})$$

*Proof.* Expanding the left hand side in Eq. (D.32), we obtain

$$\begin{aligned}
\mathbf{E} [h(\mathbf{X}_M, \alpha_2(\mathbf{X}_1), \dots, \alpha_M(\mathbf{X}_{M-1}))] &= \sum_{\mathbf{x}_M} \mathcal{L}_M(\mathbf{x}_M; \theta^*) h(\mathbf{x}_M, \alpha_2(\mathbf{x}_1), \dots, \alpha_M(\mathbf{x}_{M-1})) \\
&= \sum_{\substack{\mathbf{x}_M \\ \alpha_k(\mathbf{x}_{k-1}) = \alpha_k^* \forall k}} \mathcal{L}_M(\mathbf{x}_M; \theta^*) h(\mathbf{x}_M, \alpha_2(\mathbf{x}_1), \dots, \alpha_M(\mathbf{x}_{M-1})) \\
&\quad + \sum_{\substack{\mathbf{x}_M \\ \alpha_k(\mathbf{x}_{k-1}) \neq \alpha_k^* \exists k}} \mathcal{L}_M(\mathbf{x}_M; \theta^*) h(\mathbf{x}_M, \alpha_2(\mathbf{x}_1), \dots, \alpha_M(\mathbf{x}_{M-1})) \\
&= \sum_{\substack{\mathbf{x}_M \\ \alpha_k(\mathbf{x}_{k-1}) = \alpha_k^* \forall k}} \prod_{m=1}^M F_m(x^{(m)}; \alpha_m^*, \theta^*) h(\mathbf{x}_M, \alpha_2^*, \dots, \alpha_M^*) \\
&\quad + \sum_{\substack{\mathbf{x}_M \\ \alpha_k(\mathbf{x}_{k-1}) \neq \alpha_k^* \exists k}} \mathcal{L}_M(\mathbf{x}_M; \theta^*) h(\mathbf{x}_M, \alpha_2(\mathbf{x}_1), \dots, \alpha_M(\mathbf{x}_{M-1})) \\
&= \mathbf{E} [h(\mathbf{Y}_M, \alpha_2^*, \dots, \alpha_M^*)] \\
&\quad + \sum_{\substack{\mathbf{x}_M \\ \alpha_k(\mathbf{x}_{k-1}) \neq \alpha_k^* \exists k}} \mathcal{L}_M(\mathbf{x}_M; \theta^*) h(\mathbf{x}_M, \alpha_2(\mathbf{x}_1), \dots, \alpha_M(\mathbf{x}_{M-1})) \\
&\quad - \sum_{\substack{\mathbf{x}_M \\ \alpha_k(\mathbf{x}_{k-1}) \neq \alpha_k^* \exists k}} \prod_{m=1}^M F_m(x^{(m)}; \alpha_m^*, \theta^*) h(\mathbf{x}_M, \alpha_2^*, \dots, \alpha_M^*). \tag{D.33}
\end{aligned}$$

The above expression yields the following inequality

$$\begin{aligned}
&|\mathbf{E} [h(\mathbf{X}_M, \alpha_2(\mathbf{X}_1), \dots, \alpha_M(\mathbf{X}_{M-1}))] - \beta| \\
&\leq |\mathbf{E} [h(\mathbf{Y}_M, \alpha_2^*, \dots, \alpha_M^*)] - \beta| \\
&\quad + \sum_{\substack{\mathbf{x}_M \\ \alpha_k(\mathbf{x}_{k-1}) \neq \alpha_k^* \exists k}} \mathcal{L}_M(\mathbf{x}_M; \theta^*) |h(\mathbf{x}_M, \alpha_2(\mathbf{x}_1), \dots, \alpha_M(\mathbf{x}_{M-1}))| \\
&\quad + \sum_{\substack{\mathbf{x}_M \\ \alpha_k(\mathbf{x}_{k-1}) \neq \alpha_k^* \exists k}} \prod_{m=1}^M F_m(x^{(m)}; \alpha_m^*, \theta^*) |h(\mathbf{x}_M, \alpha_2^*, \dots, \alpha_M^*)| \\
&\leq |\mathbf{E} [h(\mathbf{Y}_M, \alpha_2^*, \dots, \alpha_M^*)] - \beta| + \gamma \sum_{\substack{\mathbf{x}_M \\ \alpha_k(\mathbf{x}_{k-1}) \neq \alpha_k^* \exists k}} \left( \mathcal{L}_M(\mathbf{x}_M; \theta^*) + \prod_{m=1}^M F_m(x^{(m)}; \alpha_m^*, \theta^*) \right), \tag{D.34}
\end{aligned}$$

where  $\gamma$  is the upper bound of  $h$ . The convergence of amplified levels implies that for all  $\epsilon > 0$  there exists  $N^* \in \mathbb{N}$  such that

$$P[\alpha_k(\mathbf{X}_{k-1}) = \alpha_k^* \forall k] = \sum_{\substack{\mathbf{x}_M \\ \alpha_k(\mathbf{x}_{k-1}) = \alpha_k^* \forall k}} \mathcal{L}_M(\mathbf{x}_M; \theta^*) = \sum_{\substack{\mathbf{x}_M \\ \alpha_k(\mathbf{x}_{k-1}) = \alpha_k^* \forall k}} \prod_{m=1}^M F_m(x^{(m)}; \alpha_m^*, \theta^*) > 1 - \frac{\epsilon}{2\gamma}, \tag{D.35}$$

for all  $N > N^*$ . Combining Eqs. (D.34), (D.35) and the assumption for the convergence of  $\mathbf{E} [h(\mathbf{Y}_M, \alpha_2^*, \dots, \alpha_M^*)]$ , we obtain Eq. (D.32).  $\square$

## E. Additional experiment

We provide additional results to confirm the asymptotic property of our estimator in a more noisy setting.

---

Here, all settings except for the noise levels are the same as Section IV A, and the depolarization noise is set to  $p_s = 1$  and  $p_q = 0.90$ . In Fig. 7, we can confirm that the RMSE achieves the CCR bound (also QCR bound) sufficiently in  $N = 500$  as in Section IV A.

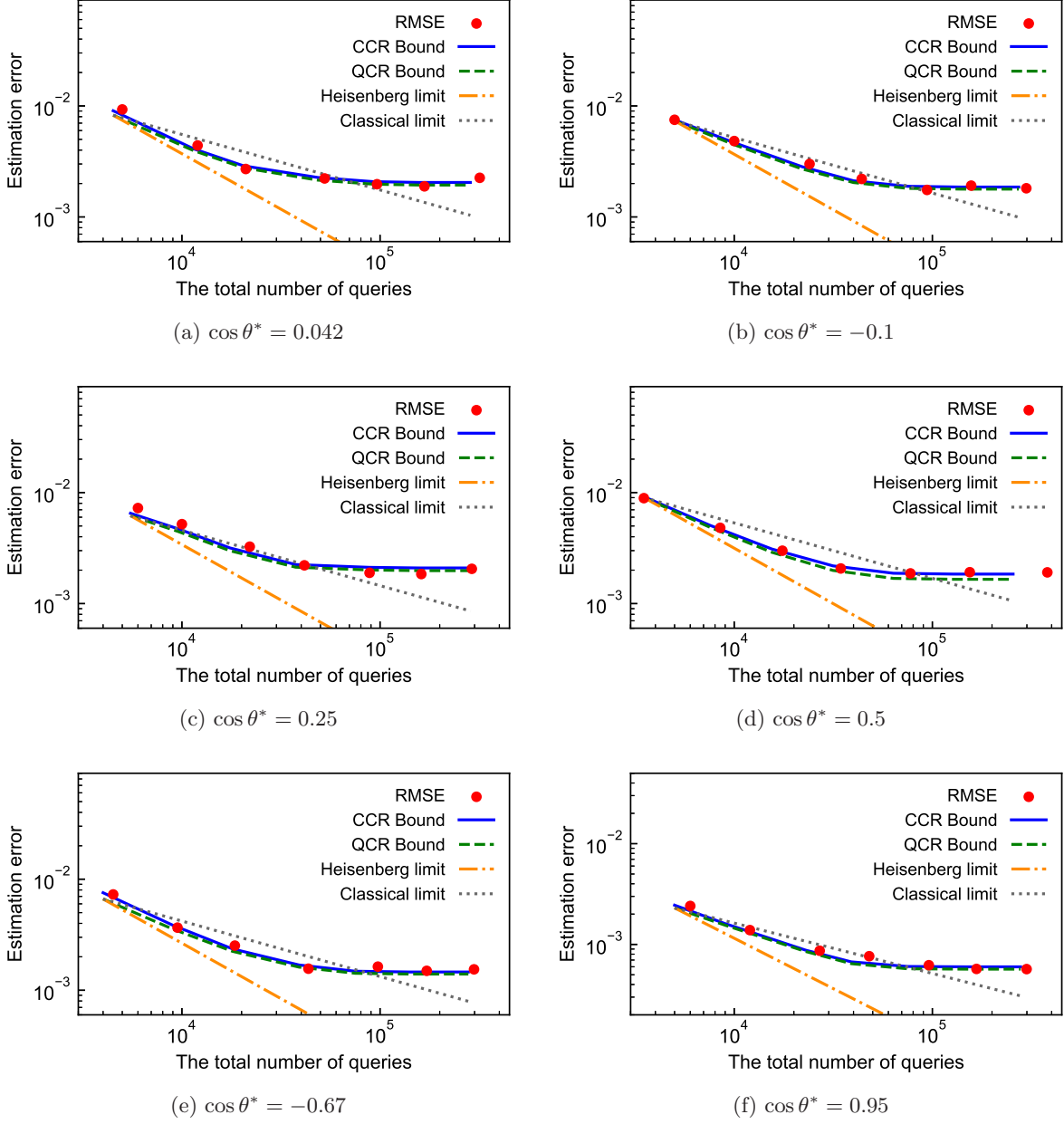


FIG. 7. The estimation error of  $\langle \mathcal{O} \rangle = \cos \theta^*$  and the total number of queries for several target values (a)–(f). The root mean squared error (RMSE) of the estimator  $\cos \hat{\theta}$  is evaluated by 200 trials, and the red plots correspond to  $M = 3, 4, \dots, 9$  from left to right. Since  $N_q$  defined in Eq. (40) is a random variable in our method, the RMSE is plotted as a function of the maximum value of  $N_q$  in 200 trials. The blue solid and green dashed lines represent the asymptotic values of CCR/QCR bounds obtained from the corresponding classical/quantum Fisher information  $\mathcal{I}_{c/q, \text{tot}}^*(\theta^*)$ , respectively. The orange dash-dotted and gray dotted lines represent the Heisenberg limit and the classical limit, respectively.